Use of national forest inventory data to develop stand density driven models for understorey shrubs and overstorey fuel variables and associated temporal dynamics in commercial plantations

Fernando CASTEDO-DORADO[a*]

Ana Daría RUIZ-GONZÁLEZ[b]

José Antonio VEGA HIDALGO[c]

Stéfano ARELLANO-PÉREZ[d]

Juan Gabriel ÁLVAREZ-GONZÁLEZ[b]

[a] DRACONES Research Group. Departamento de Ingeniería y Ciencias Agrarias, Universidad de León. Escuela de Ingeniería Agraria y Forestal, Avda. de Astorga s/n, 24401 PONFERRADA (León), Spain. E-mail: fcasd@unileon.es. Phone: + 0034 987442078. Fax: + 0034 987442070

[b] Unidad de Gestión Ambiental y Forestal Sostenible (UXAFORES), Departamento de Ingeniería Agroforestal, Escuela Politécnica Superior de Ingeniería, Universidad de Santiago de Compostela. R/ Benigno Ledo, Campus universitario, 27002 LUGO, Spain. E-mail: anadaria.ruiz@usc.es; juangabriel.alvarez@usc.es.

[c] Centro de Investigación Forestal de Lourizán, Xunta de Galicia, PO Box 127, 36080 PONTEVEDRA, Spain. E-mail: josea2.vega@gmail.com

[d] AGRESTA Sociedad Cooperativa, c/ Duque de Fernán Nuñez 2, 28012 Madrid, Spain. E-mail: sarellano@agresta.org

* **Corresponding author**

Abstract

Biomass tends to accumulate both in overstorey and understorey layers of forests growing in productive areas. The rapid growth of forest plantations established in productive areas can thus also lead to the creation of fire-prone landscapes. In this study, we assessed the extent to which overstorey stand density determines current values of the fine shrub fuel load (W_{shr_G1}) in the understorey and also two major canopy fuel characteristics related to crown fire activity -canopy base height (*CBH*) and canopy bulk density (*CBD*)- and the temporal dynamics of these. For this purpose, we developed two types of models for the three fuel complex variables: i) extreme response models, to define the upper limit of W_{shr_G1} and *CBD* and the lower limit of *CBH*, the values of which may depend on stand density; and ii) dynamic models, to estimate the probability of increasing fuel loads and rate of change when a more hazardous situation is predicted. Data were obtained from 8087 plots, measured in the third, fourth and fifth Spanish National Forest Inventories, in plantations dominated by the major commercial species in northern Spain (*Pinus pinaster*, *Pinus radiata*, *Pinus sylvestris* and *Eucalyptus globulus*).

The extreme response models generally explain more than 60% of the observed variability in the three fuel complex variables. According to these models, maximum shrub fuel load and *CBD* and minimum *CBH* in stands of the four tree species were limited by stand basal area, with different responses by different species.

The dynamics of the fuel complex variables were determined by canopy cover, estimated as a proxy for stand density. The use of a two-step regression approach enabled realistic modelling of the dynamics of the fuel complex variables, allowing for a decrease in the shrub fuel biomass and in *CBD* between two time points. The dynamic models developed are age-independent and are therefore useful for practical

applications because they can be applied to any stand without the need to know the stand age.

Overall, the study findings provide insights into the complex relationship between both understorey and overstorey fuels and stand density in commercial plantations. As assessment of forest fuel complex variables is a prerequisite for most fire management activities, the study findings have important implications for forest and fuel management and planning in the region.

Keywords: fuel complex variables, extreme response models, fuel dynamics, fuel management, wildfires

1. INTRODUCTION

Wildfire activity depends on the availability of biomass, which is regulated by land productivity (Pausas and Paula, 2012). Northern Spain is a highly productive forest area owing to the suitability of conditions for tree growth (Aguirre et al., 2022) and it is by far the most important region in Spain in terms of timber production (Gómez-García, 2020). It is also considered a highly productive forest region in the European (Verkerk et al., 2015) and global (Del Grosso et al., 2008) contexts. Forest plantations have been widely established throughout the north of Spain since the middle of the 20th century to meet increasing demands for timber and other forest products. These commercial plantations primarily consist of four species: *Pinus pinaster* Ait (maritime pine), *Pinus radiata* D. Don (Monterey pine), *Pinus sylvestris* L. (Scots pine) and *Eucalyptus globulus* Labill. (blue gum). In the last two decades, *Eucalyptus nitens* (Deane and Maiden) Maiden has also been added to this group of highly productive species. Plantations of the above-mentioned five major species currently cover more than 40% of the total wooded area (i.e. 1M ha of 2.5 Mha), according to the fourth Spanish Forest Inventory (MARM, 2011; MAGRAMA, 2012a, 2012b, 2013). These plantations also play a key role in the Spanish forestry sector, representing *circa* 75% of the average annual timber volume harvested in the whole of Spain (MAPA, 2019a). Moreover, the existence of these plantations has led to northern Spain being one of the regions in Europe with the highest intensity of forest harvesting (Levers et al., 2014).

Northern Spain is also one of the areas with the highest wildfire frequency at national and continental scales (Oliveira et al., 2012; San-Miguel-Ayanz et al., 2018; MAPA, 2019b). This can be explained by three concurrent factors: the high ignition rate, usually directly or indirectly related to human activities; the existence of periods of drought throughout the year, which increases fuel flammability; and the high vegetation

productivity, which promotes biomass accumulation both in the overstorey and understorey (Légaré et al., 2001). Hence, while commercial forest plantations contribute to the local economy and provide timber resources, they also bring about challenges related to the creation of fire-prone landscapes (Cruz et al., 2008).

Forest structure and fuel loads strongly influence the rate of spread and intensity of wildfire (e.g. Pyne et al., 1996; Graham, et al. 2004; Rego et al., 2021), and characterization of the structural vegetation components is therefore essential for fire risk assessment (e.g. Calkin et al., 2010; Scott et al., 2013; Thompson et al., 2015; Chuvieco et al., 2023). In forest ecosystems, the fuel bed is usually structured in ground, surface and canopy fuel layers, each of which exhibits vertical stratification (Keane, 2015). In temperate forests, the understorey comprises one of the main components of the surface fuel layer. Forest understorey refers to vegetation that grows beneath the forest canopy, and it includes a variety of species, including shrubs, herbaceous plants and ferns (Helms, 1998). Accumulation of understorey fuel in general, and shrub fuel in particular, can lead to a higher fireline intensity of surface fire (Byram, 1959; Fernandes et al., 2004, 2009), greater crown fire hazard (Agee and Skinner, 2005) and therefore an increased probability of tree damage and mortality (Scott and Reinhardt, 2001). High shrub fuel loads can also increase the probability of forest stands being affected by wildfire, as observed in the Iberian Peninsula (Botequim et al., 2013; Nunes et al., 2019).

Forest overstorey refers to the uppermost layer of vegetation in a forest, and in commercial plantations it is typically composed of trees planted in rows or grids with a consistent spacing pattern to optimize ground occupancy. Canopy fuels comprise the biomass of the overstorey layer and can be roughly characterized by two structural variables: canopy base height (*CBH*) and canopy bulk density (*CBD*). Both of these

variables affect the initiation and spread of crown fires (van Wagner, 1977; Cruz et al., 2004, 2006; Alexander and Cruz, 2011), and they are therefore critical for predicting fire behaviour (Cruz et al., 2005, 2008).

In commercial plantations, both overstorey and understorey layers are usually involved in the propagation phase of wildfires. Moreover, complex interactions between the overstorey and understorey layers are known to occur (Balandier et al., 2022). Overstorey trees play a crucial role in shaping the structure and function of the forest ecosystem dynamics, mainly due to light interception (Messier et al., 1998; Ameztegui and Coll, 2013). Other mechanisms whereby the overstorey controls understorey development are also important, including direct competition via the accumulation of a dense litter layer (White et al., 1991), competition for water and nutrients (e.g. Uresk and Severson, 1989) and allelopathy, the latter particularly in non-woody species (e.g. da Silva et al., 2015).

The practical quantification of both understorey fuel loads and canopy fuel characteristics requires the use of indirect estimation methods such as allometric equations (e.g. Keane et al., 2005; Vega et al., 2022a; Vega et al., 2022b). Fernandes et al. (2002) developed a model for estimating the understorey fine fuel load (diameter <0.6 cm, hereafter *G*1) in *P. pinaster* stands in northern Spain, using phytovolume as a predictor. Nevertheless, application of the model is limited to situations where species of the genera *Cytisus* or *Cistus* do not dominate the understorey. More recently, Vega et al. (2022a) developed two equation systems for the major pine species in NW Spain (*P. pinaster*, *P. radiata* and *P. sylvestris*), one of which uses understorey and overstorey variables as regressors for estimating understorey fuel components by size and condition (live and dead) and the other of which only uses overstorey variables. The suitability of a system of allometric equations that enables

prediction of understorey fuel loads using only understorey area-based attributes, which allows rapid estimation of shrub loads without requiring a tree inventory, remains to be explored. Of all the understorey fuel load components, fine shrub fuel load (W_{shr_G1}) is particularly important as it contributes most to fire spread (Rothermel, 1972; Pyne et al., 1996; Scott and Reinhardt, 2001).

This system of allometric equations would benefit from being able to be used with data from large-scale sources of information such as the Spanish National Forest Inventories (SNFIs), in which understorey area-based attributes (the composition of woody shrub layer, the percent cover and the mean height) are measured (Alberdi et al., 2017; Sánchez-Pinillos et al., 2021). As tree species, diameter at breast height and total height are also measured in all trees in the plots in SNFIs, species-specific equations can be used to estimate the canopy fuel structural characteristics (*CBH* and *CBD*) at plot level. In a database as extensive as that provided by the SNFI, and considering the vast geographical area comprising northern Spain, many factors other than the overstorey species and density can modulate the understorey fuel load and canopy fuel characteristics: the plant species composition of the understorey community, the time since the last disturbance of the understorey, management of the overstorey, the plantation age and site quality (e.g. Parresol et al., 2012). Indeed, preliminary analysis of SNFI data has shown that, at plot level, the calculated values of the fuel complex descriptors W_{shr_G1}, *CBH* and *CBD* vary widely in an increasing gradient of stand density. In this type of data distribution, the so-called extreme response models will represent the potential effects of overstorey stand density on understorey shrub fuel load and canopy fuel characteristics. Extreme response models have been used successfully to quantify thresholds or limits, and the extent to which a predictor constrains a response variable (McKenzie et al., 2000). From the point of view of fire risk

assessment, these models can be used to represent the worst-case-scenarios in wildfire simulations, and they are therefore can be preferred over the mean response models because the latter do not fully capture the fire risk potential.

One shortcoming of the extreme response models is that they represent a static approach, and therefore they fail to predict rates of change. In other words, they do not consider the dynamics of the fuel complex associated with stand growth and the related effects of stand density management. As models that quantitatively describe the dynamics of the forest fuel complex over time are suitable for permanent updating of fire risk assessment to assist fuel management decisions (Bilgili and Methven, 1994; Bilgili, 2003; Fernandes and Rigolot 2007), development of dynamic models for projecting W_{shr_G1}, *CBH* and *CBD* over time is advisable.

Few studies have conducted detailed evaluations of the dynamics of fuel complex characteristics in forest plantations (Bilgili and Methven, 1994; Ruiz-González et al., 2015; Botequim et al., 2015, the latter for western Iberian Peninsula). Botequim et al. (2015) developed two models from Portuguese NFI data to describe the temporal dynamics of shrub biomass in the forest understorey in forests in Portugal. These models assume that shrub biomass tends to increase with time since disturbance until reaching an asymptote, which represents the maximum (steady-state) shrub biomass for a given site. Thus, the models developed by Botequim et al. (2015) do not consider the alternative that the shrub load may decrease over time due to shrub mortality, driven by overstorey competition. On the other hand, Ruiz-González et al. (2015) developed models that enable prediction of the rates of change in *CBH* and *CBD* in maritime pine stands. Although these models take thinning effects into consideration, the overstorey stand age must be known, and this information is not always readily available.

Therefore, development of new models for fuel complex variables that are more

187 biologically realistic (e.g. assuming the possibility of a decrease in the shrub load due to
188 mortality, driven by overstorey competition) and also age-independent (i.e. more
189 generalizable, without the need to know stand age) is advisable.
190 SNFIs collect information from each permanent plot over a period of approximately 10
191 years, enabling quantification of rates of change of the fuel complex variables between
192 successive inventories. Moreover, the measurement of both overstorey and understorey
193 attributes in each inventory enables the potential influence of stand density to be
194 considered in the explanatory ability of the dynamic models.
195 Consequently, the objectives of the study were as follows: (i) to construct additive shrub
196 fuel biomass equations from area-based understorey metrics; (ii) to develop extreme
197 response models of W_{shr_G1}, *CBD* and *CBH* using a proxy for overstorey stand density;
198 and (iii) to develop models to estimate the changes in these variables towards higher fire
199 hazard conditions during a certain time interval, including the potential effect of stand
200 density. As the effect of stand density may mainly depend on how much light the
201 overstorey species intercept according to their architectural structure (e.g. Balandier et
202 al., 2022), in addition to a general model for all species, different models were fitted for
203 each species for the latter two objectives.
204 All of these models are expected to be helpful for supporting forest and fire
205 management and planning in fire prone commercial plantations.
206

207 **2. MATERIAL AND METHODS**

208 **2.1. Study area, overstorey species and inventory plots**

209 The study area corresponds to the Atlantic area of northern Spain, including the regions
210 of Galicia, Asturias, Cantabria and the two coastal provinces of the Basque Country
211 (Vizcaya and Guipúzcoa). Most of the area occupied by these regions is included in the

Eurosiberian biogeographic region, roughly characterized by mild climate and less than two months of dryness (Moreno et al., 1990). These mild climate conditions, in terms of thermal regime and water availability, favour high site productivity.

The data used were obtained from the third Spanish National Forest Inventory (SNFI-3), the fourth Spanish National Forest Inventory (SNFI-4) and the Forest Inventory of productive species in the north of Spain (SNFI-5). The inventories were carried out in the study area between 1997 and 2006 (SNFI-3), between 2009 and 2011 (SNFI-4) and during 2018 (SNFI-5). The SNFI project maintains a systematic network of sample plots established at the intersections of a 1-km × 1-km UTM grid throughout Spain to provide continuously updated information regarding the status of forest resources nationwide (Alberdi Asensio et al., 2010).

The present study focuses on the most productive commercial species in the region, and the forests measured in the SNFI therefore included four pure, even-aged forest types: maritime pine (*P. pinaster*), radiata pine (*P. radiata*), Scots pine (*P. sylvestris*) and blue gum (*E. globulus*). Shining gum (*E. nitens*) was not included because of the low availability of SNFI plots for this species. Sample plots in which the basal area of one of the four selected species was lower than 90% were rejected. Additionally, SNFI plots with explicit signs (as judged by forest surveyors) of recent human activity in the understorey (e.g. bush clearing) or fire occurrence were excluded from the analysis. A total of 8087 sample plots (3439 from SNFI-3; 3545 from SNFI-4 and 1103 from SNFI-5) were finally selected (Figure 1).

The most common vegetation in the forest understorey is composed of evergreen woody species communities dominated by the genera *Ulex* and *Erica*, followed by *Daboecia, Calluna*, *Cistus*, *Pterospartum*, *Cytisus* and *Halimium*. Of the non-woody shrubs species, bracken fern (*Pteridium aquilinum* L.) and brambles (*Rubus* spp.) are

237 particularly common, especially in humid and more productive sites. However, the
238 SNFIs do not include ferns, as the characteristics of these plants are difficult to assess
239 owing to the different physiological states in which they can be found throughout the
240 year.

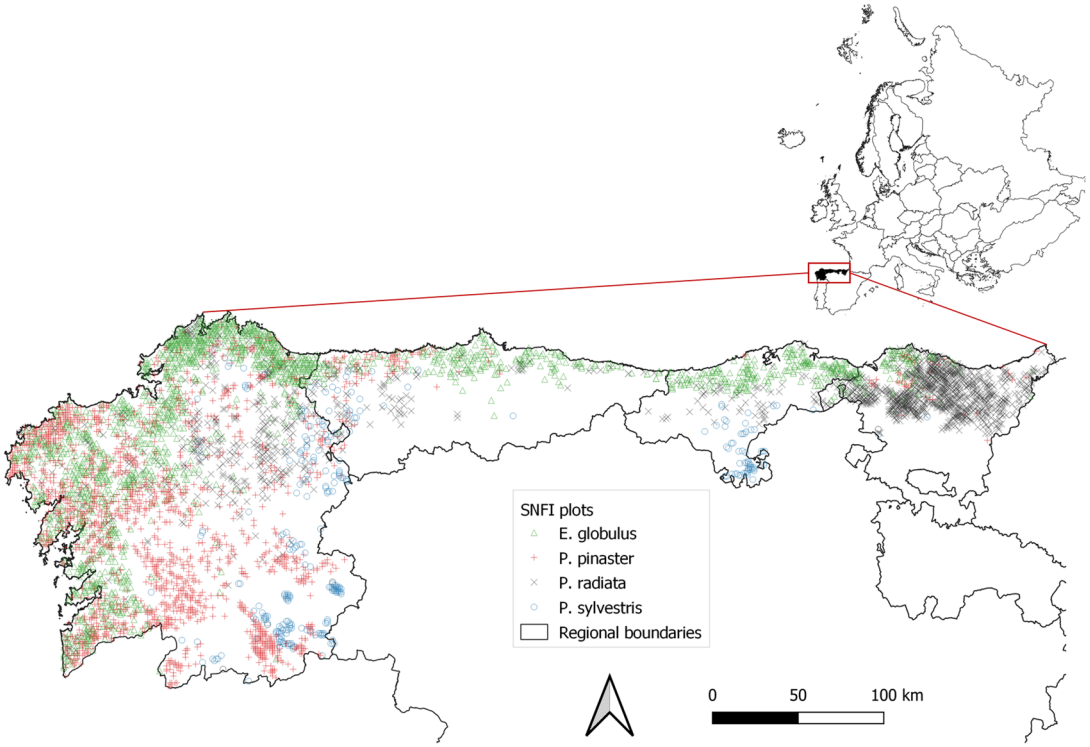

241 Figure 1. Spatial distribution of the SNFI plots in the study area where *E. globulus*, *P.*
242 *pinaster*, *P. radiata* and *P. sylvestris* dominate the overstorey (stand basal area,
243 $G > 90\%$). The map is based on the distribution of the plots in SNFI-4.
244
245 **2.2. Overstorey variables**
246 The sample plots each consist of four circular concentric subplots of radii 5, 10, 15 and
247 25 m. Diameter at breast height (*dbh*) and total height were measured in trees selected
248 on the basis of diameter and distance from the plot centre (*dbh* ≥ 42.5 cm for plot radius
249 25 m; *dbh* ≥ 22.5 cm for plot radius 15m; *dbh* ≥ 12.5 cm for plot radius 10 m and *dbh* ≥
250 7.5 cm for plot radius 5m). Diameters were measured with a graduated tree caliper, to

the nearest 0.1 cm, in two perpendicular directions. Tree height was measured with a hypsometer, to the nearest 0.1 m. The number of stems per hectare (*N*), basal area (*G*), mean diameter ($\bar{d}$), mean height ($\bar{h}$) and dominant height (*H*, defined as the mean height of the 100 thickest trees per hectare) were calculated from the tree variable measurements, taking into account the number of trees per hectare that each selected tree represents in the inventory, according to the subplot radius.

Crown diameter (*cd*) and crown length (*cl*) of each tree were estimated using the species-specific equations proposed by Nunes et al. (2020) and fitted using information from four sample trees systematically selected in each sample plot of the SNFI-2 to complete a database with more than 255,000 sample trees covering the distribution area of all the forest species in Spain and all combinations of age, stand density and site qualities.

Canopy Cover (*CC*) and Canopy Base Height (*CBH*), the latter defined as the mean value of the crown base height of each tree, were estimated for each sample plot from the *cd* and *cl* estimates, respectively, for each tree.

The Canopy Fuel Load (*CFL*), defined here as the biomass of needles and fine twigs of diameter less than 0.5 cm, was estimated by aggregation of the dry weight of these fractions of each tree. The dry weights were estimated using the compatible systems of tree biomass equations developed for maritime pine, radiata pine and blue gum in Galicia (Diéguez-Aranda et al. 2009) and the equations proposed for Scots pine by Montero et al. (2005), with the corrections for fine biomass proposed by Fernandez-Alonso et al. (2013). Individual trees of another species were observed in the sample plots and represented 0.62 % of the selected trees. Surrogate species selected on the basis of similarities in crown structure were used to estimate crown variables and fine fuel biomass of these species. Canopy Bulk Density (*CBD*) was estimated as the ratio

between *CFL* and canopy length, which is defined as the difference between the mean height ($\bar{h}$) and *CBH*.

2.3. Understorey variables

The percent cover and the mean height of each species or group of species of the understorey were recorded in the 10 m radius subplot in each sample plot (Alberdi et al., 2017). Percent cover was assessed visually, and mean height was measured with graduated pole, to the nearest 0.1 m.

Total shrub cover (Cov_{shr}) was estimated in each sample plot by summing the percent cover of the individual species (or group of species) in the sample plot. Mean shrub height ($\overline{h_{shr}}$) was calculated as the weighted (by cover) average of the species (or group of species) height measurements.

In the study area, systems of compatible equations have been developed that allow estimation of the fuel load of understorey in stands of the three pine species studied (Vega et al., 2022a). However, both shrub variables and stand variables such as $\bar{h}$ and *N* are required as input variables. As the objective of this study was to assess the effect of the overstorey on the development and evolution of the understorey, we decided to fit a compatible system of equations to estimate understorey fuel loads based exclusively on shrub variables (Cov_{shr} and $\overline{h_{shr}}$) and using the same database as in Vega et al. (2022a), but excluding those plots in which ferns and brambles dominate the understorey or where understorey is absent. The description of the database used to fit these equations, the models and methodology used, the results obtained, and their discussion are provided as Supplementary material.

The mean, maximum, minimum values and standard deviations for the main stand, canopy and understorey variables are shown in Table 1.

300 **Table 1**. Mean value and standard deviation of the main overstorey and understorey
301 variables distinguished by overstorey species. Values of W_{shr_G1} were estimated using
302 the equations described in Supplementary material.

Variable	Statistic	*P. pinaster* n = 2756	*P. radiata* n = 2030	*P. sylvestris* n = 441	*E. globulus* n = 2860
$\bar{d}$	Mean	22.32	26.58	18.96	15.63
(cm)	St. dev.	8.95	11.49	6.80	6.20
$\bar{h}$	Mean	12.82	17.45	9.80	16.28
(m)	St. dev.	4.90	6.91	3.99	4.84
N	Mean	562.77	563.80	863.68	879.44
(stems/ha)	St. dev.	498.70	407.96	619.00	594.45
G	Mean	20.83	27.76	23.54	18.07
(m^2/ha)	St. dev.	15.62	16.96	16.30	13.77
H	Mean	15.50	20.48	11.07	21.09
(m)	St. dev.	5.98	7.73	4.27	7.53
CC	Mean	46.47	69.61	85.89	50.26
(%)	St. dev.	33.06	35.77	54.66	35.46
CBH	Mean	3.74	5.70	1.81	5.11
(m)	St. dev.	1.30	3.83	0.52	1.07
CFL	Mean	0.56	0.80	1.02	0.65
(kg/m^2)	St. dev.	0.44	0.47	0.67	0.49
CBD	Mean	0.058	0.067	0.130	0.056
(kg/m^3)	St. dev.	0.039	0.035	0.079	0.036
Cov_{shr}	Mean	80.43	75.66	72.36	74.22
(%)	St. dev.	46.73	44.34	43.35	43.96
$\overline{h_{shr}}$	Mean	77.76	81.49	74.08	89.21
(cm)	St. dev.	41.13	47.35	39.36	47.42
W_{shr_G1}	Mean	1.01	0.96	0.92	1.01
(kg/m^2)	St. dev.	0.71	0.72	0.70	0.77

303

304 **2.4. Modelling approaches**

305 *2.4.1 Models including the effect of stand density for estimating surface and canopy*
306 *fuel-related variables*

307 Two types of models were developed to assess the effect of stand density on the three
308 fuel complex variables considered here (W_{shr_G1}, *CBH* and *CBD*): 1) extreme response
309 models, which are static models; and 2) dynamic models, to estimate the probability that
310 these variables will evolve towards conditions implying a greater risk of surface and/or

311 crown fires and also the rate of change of the variables when a more hazardous situation
312 is predicted.
313 These two types of models were fitted independently to each of the four species
314 analyzed and for all species together.
315 *Extreme response models*
316 To fit the extreme response curves (i.e. to model an upper limit of W_{shr_G1} and *CBD* and
317 a lower limit of *CBH* whose value is regulated by stand density), the stand basal area
318 (*G*) was included as a predictor variable as it has produced better results than other
319 stand density surrogates (*N*, *SDI* and *CC*) in terms of goodness-of-fit (minimizing the
320 sum of squares of the errors, results not shown) and it is easy to measure in the field.
321 The values corresponding to the 99th percentile of the distribution of W_{shr_G1} and *CBD*
322 and those corresponding to the 1st percentile for *CBH* were determined at intervals of 2
323 m^2/ha within the observed range of values of *G*. A weighted Multivariate Adaptive
324 Regression Splines (MARS) approach was used to fit the model to the percentile data as
325 a function of *G* values for each species. The ratios between the observations used to
326 obtain each of the percentiles and the total number of observations were assigned as
327 weights. The nonparametric MARS technique (Friedman, 1991) constructs a non-linear
328 regression model by fitting piecewise linear regressions in distinct intervals of the
329 independent variable space.
330 *Dynamic models*
331 A two-step regression approach was used to model the dynamics of the fuel complex
332 associated with stand growth and the potential modulating effects of stand density.
333 In the first step, equations for predicting the probability of W_{shr_G1} and *CBD* increasing
334 between consecutive inventories were fitted (*CBH* values are assumed to be maintained
335 or to increase over time as recruitment is irrelevant in these pure and even-aged stands).

In the second step, transition functions were developed in order to estimate the rate of change of W_{shr_G1}, *CBD* and *CBH* between inventories. In the second step, we only considered those plots in which a change in fuel complex variables towards greater fire risk between inventories was detected.

The fit of the dynamic models requires data from two measurements of the same sample plot. We only included those plots in which the species was maintained between successive SNFIs and in which the dominant height increased in order to take into account the dynamics of the fuel complex associated with stand growth. In total, 1817 pairs of measures on the same sample plot (680 from *P. pinaster*, 456 from *P. radiata*, 132 from *P. sylvestris* and 543 from *E. globulus*) were finally fitted to the dynamic models.

As a result of stand development in the time elapsed between inventories, W_{shr_G1} and *CBD* values may increase (1, higher fire hazard) or decrease (0, lower fire hazard). Therefore, a logistic model (e.g. Monserud, 1976; Hosmer and Lemeshow, 2000) that provides estimates of probability of fire hazard increment was fitted for W_{shr_G1} and *CBD*:

$$p = \left[\frac{\exp(d_0 + d_i\, X_i)}{1 + \exp(d_0 + d_i\, X_i)}\right]^{\Delta t} \quad (1)$$

where p represents the probability that fire hazard will increase (increment in W_{shr_G1} and *CBD* values) over a time interval of Δt years, d_0 and d_i are the parameters to be estimated and X_i are the explanatory variables which characterize the stand density.

In equation (1), the probability decreases as the time interval increases and it gradually approaches zero. This assumption is biologically consistent in the case of W_{shr_G1}, because canopy cover increases as these pure and even-aged stands gradually develop, negatively affecting understorey growth. However, in the case of *CBD* it seems more plausible to assume the opposite effect, as stand growth implies an increase in the

values of *CFL* as well as less variation in canopy length (e.g. Crecente-Campo et al., 2009; Ruiz-González et al., 2015); therefore, the exponent of equation (1) was replaced with $1/\Delta t$ for this variable.

Three different alternatives were tested as independent variables of the logistic model, consisting of the value of the variable of interest in the first measurement, combined with one of the four density-related variables that are easiest to measure in the field (*N, SDI* and *G*) or estimate from field measurements (*CC*), and the combination that yielded the highest values for the classification accuracy was selected.

Once each logistic regression model was fitted, the threshold for deciding whether the estimated probability indicates higher fire risk was obtained by maximizing both the sensitivity and specificity of the model for the complete database of each species.

The transition functions were derived from the base model proposed by Bertalanffy-Richards (Bertalanffy, 1957; Richards 1959):

$$Y = f_0\,(1 - \exp\,(-f_1\,t))^{f_2} \tag{2}$$

where Y is the independent variable analyzed (W_{shr_G1}, *CBD* and *CBH*), t is the stand age (years) and f_i are the parameters to be estimated. This is a sigmoidal growth function with a horizontal asymptote equal to parameter f_1.

The first step in developing the transition function involves definition of a difference form of the base model considering two different measures of the same plot: (Y_1, t_1) and (Y_2, t_2). As both measurements correspond to the same sample plot, the f_i parameters are the same. The first expression can therefore be solved for t_1 and then substituted in the second expression, considering that $t_2 = t_1 + \Delta t$, to obtain the transition function (e.g. Tomé et al., 2006; Burkhart and Tomé, 2012) (equation 3):

$$\left.\begin{aligned} Y_1 &= f_0\,(1 - \exp\,(-f_1\,t_1))^{f_2} \\ Y_2 &= f_0\,(1 - \exp\,(-f_1\,t_2))^{f_2} \end{aligned}\right\} \Rightarrow \frac{-\ln\left(1 - \left[\frac{Y_1}{f_0}\right]^{1/f_2}\right)}{f_1} = t_1$$

$$Y_2 = f_0 \left(1 - \left[1 - \left[\frac{Y_1}{f_0} \right]^{1/f_2} \right] \exp\left(-f_1\, \Delta t\right) \right)^{f_2} \quad (3)$$

Only those pairs of measurements from the same plot in which an increase in the variable of interest (W_{shr_G1}, *CBD* and *CBH*) were observed were used to fit equation 3.

2.5. Statistical analysis

The dynamic models of change in W_{shr_G1}, *CBH* and *CBD* (equation 3) were fitted by Ordinary Least Squares (OLS) using the MODEL procedure of SAS/ETS® (SAS Institute Inc., 2004). For extreme response of W_{shr_G1}, *CBH* and *CBD*, the weighted MARS (Multivariate Adaptive Regression Splines) models were fitted using the "earth" package (Milborrow, 2023) in R software (R Core Team, 2022).

Two goodness-of fit statistics were used to check the accuracy of estimates: model efficiency (ME) and root mean square error (RMSE).

$$\mathrm{ME} = 1 - \frac{\sum_{i=1}^{n} \left(Y_i - \widehat{Y}_i\right)^2}{\sum_{i=1}^{n} (Y_i - \bar{Y})^2} \quad (4)$$

$$\mathrm{RMSE} = \sqrt{\frac{\sum_{i=1}^{n} \left(Y_i - \widehat{Y}_i\right)^2}{n-1}} \quad (5)$$

where Y_i, $\widehat{Y}_i$ and $\bar{Y}$ are the observed, predicted and mean values of the dependent variable and n is the number of observations used to fit the equation.

The parameters of the logistic models were estimated using the "optim" function of R (R Core Team, 2022) to maximize the logarithm of the likelihood function of equation (1). The best set of independent variables was obtained by using the stepwise procedure with the "step" function in R (R Core Team, 2022). The performance of the logistic models was evaluated in terms of percentage of concordant pairs.

401 **3. RESULTS**

402 **3.1. Models including the effect of stand density for estimating surface and canopy**

403 **fuel-related variables**

404 *Extreme response models*

405 The mathematical expressions of the MARS models fitted to estimate the extreme

406 response of W_{shr_G1}, *CBH* and *CBD* as a function of *G* for each of the four overstorey

407 species and for all species together, as well as the values of the goodness-of-fit

408 statistics, are shown in Table 2. The corresponding scatter plots and the lines

409 representing the extreme response MARS model are shown in Figure 2.

410

411 **Table 2**. Mathematical expressions of the MARS models fitted to characterize the

412 extreme response models of W_{shr_G1} (99th percentile); *CBD* (99th percentile) and *CBH*

413 (1st percentile) as a function of *G*.

Fine shrub fuel load (W_{shr_G1}, kg/m^2)			
Species	Equation	ME	RMSE
P. pinaster	$Y = 2.2932 + 0.0132(42 - G) - 0.0366(G - 42)$	0.6791	0.1915
P. radiata	$Y = 2.6356 - 0.0157(G - 30)$	0.2726	0.2789
P. sylvestris	$Y = 2.3402 - 0.0390(G - 18)$	0.7214	0.3099
E. globulus	$Y = 2.2268 + 0.0155(52 - G) - 0.0670(G - 52)$	0.5818	0.2234
All species	$Y = 2.1397 + 0.0107(76 - G) - 0.0747(G - 76)$	0.6109	0.2476
Canopy bulk density (*CBD*, kg/m^3)			
Species	Equation	ME	RMSE
P. pinaster	$Y = 0.0970 + 0.0023(G - 18) - 0.0052(18 - G)$	0.9586	0.0104
P. radiata	$Y = 0.1252 + 0.0017(G - 30) - 0.0044(24 - G)$	0.8877	0.0143
P. sylvestris	$Y = 0.3204 - 0.0083(30 - G)$	0.6513	0.0609
E. globulus	$Y = 0.0980 + 0.0020(G - 16) - 0.0056(16 - G)$	0.9616	0.0086
All species	$Y = 0.1790 + 0.0014(G - 16) - 0.0101(16 - G)$	0.8660	0.0242
Canopy base height (*CBH*, m)			
Species	Equation	ME	RMSE
P. pinaster	$Y = 2.5828 + 0.0283(G - 30) - 0.0551(30 - G)$	0.9238	0.2029
P. radiata	$Y = 1.5746 + 0.0662(G - 24) - 0.0433(24 - G)$	0.8735	0.3858
P. sylvestris	$Y = 1.2806 + 0.0269(G - 30) - 0.0432(18 - G)$	0.8321	0.1737
E. globulus	$Y = 3.6626 + 0.0243(G - 16) - 0.1429(16 - G)$	0.8955	0.3040
All species	$Y = 3.3251 + 0.2298(G - 82) - 0.0316(82 - G)$	0.8434	0.2231

414

As expected, the models show that the W_{shr_G1} values tend to decrease and *CBD* and *CBH* values to increase as *G* increases (Figure 2). Overall, the best results were obtained for *CBH* and *CBD*, and the observed variability explained by the extreme response models was 84% and 86%, respectively, for all of the species considered together. The W_{shr_G1} extreme response models generally yielded poorer goodness-of-fit statistics, with percentages of explained observed variability varying between 58 and 72%, except for *P. radiata*, for which the percentage was much lower (27%).

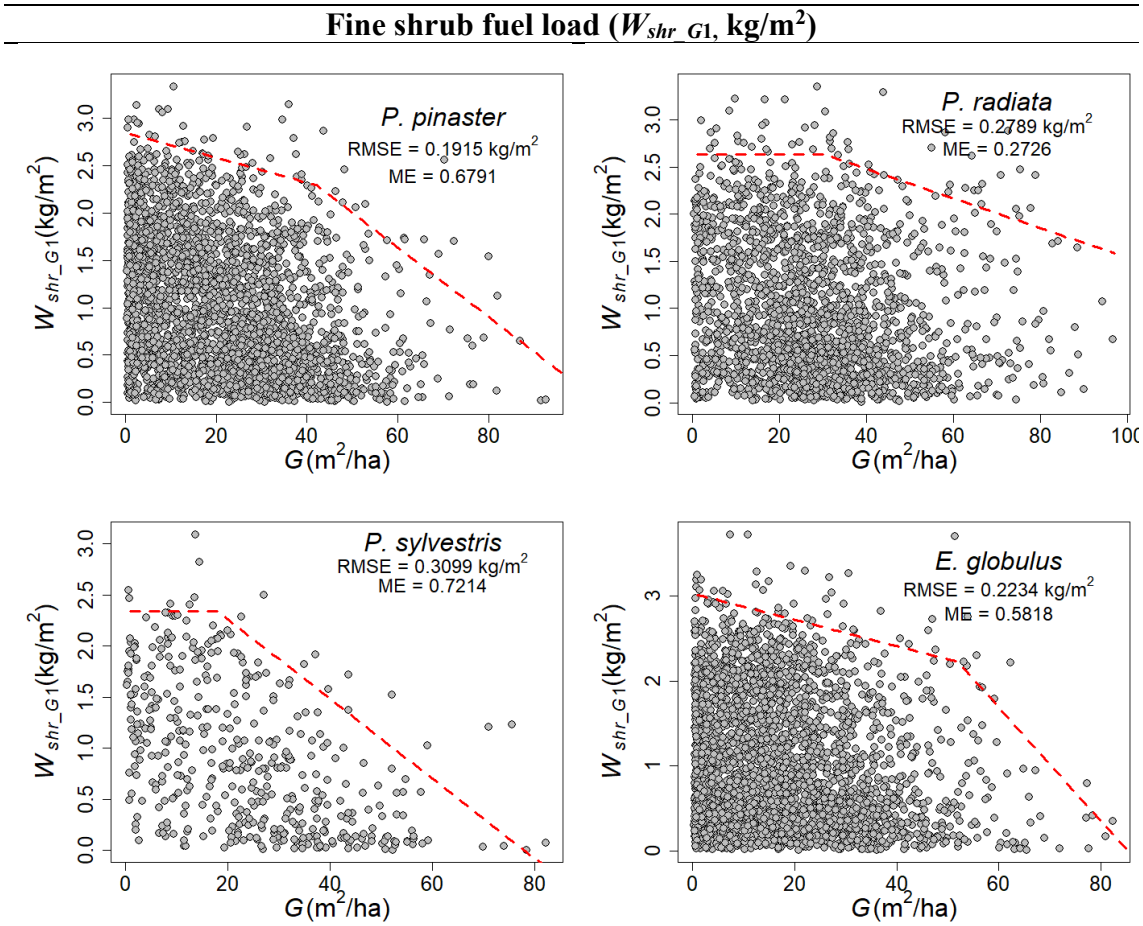

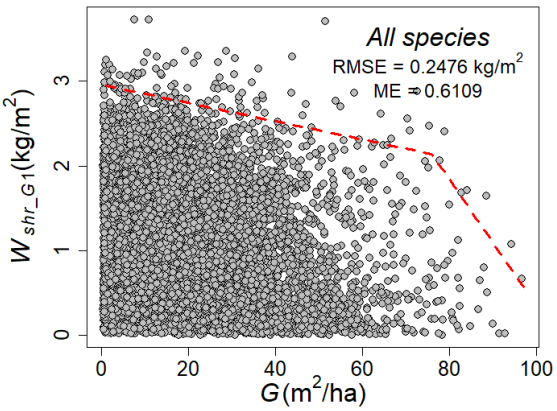

Canopy bulk density (*CBD*, kg/m^3)

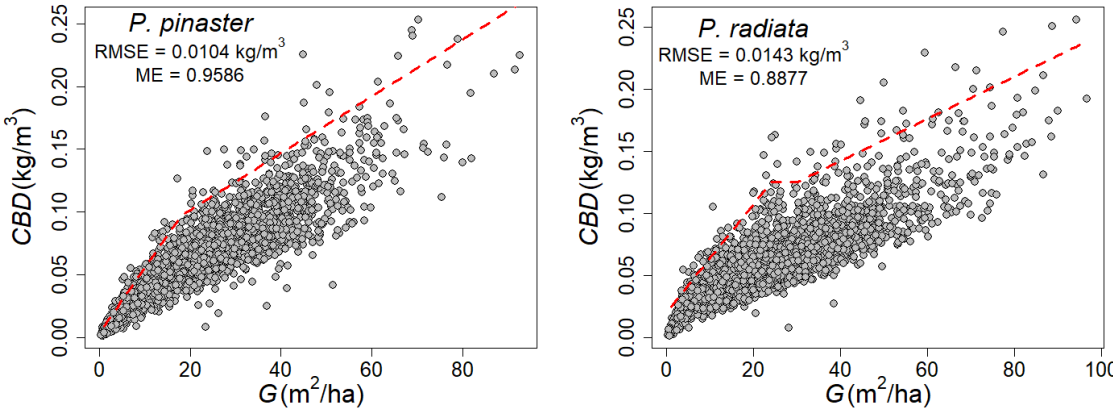

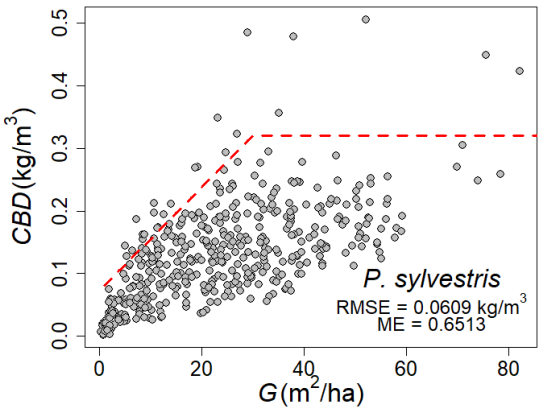

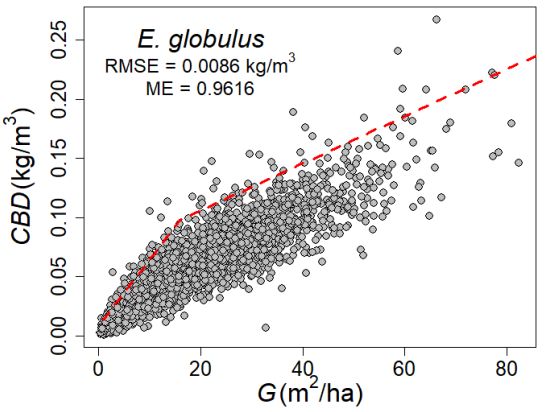

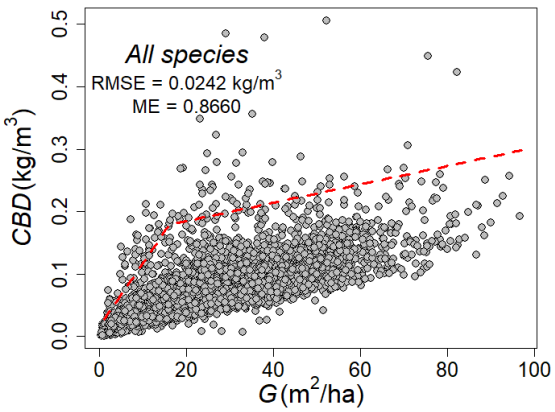

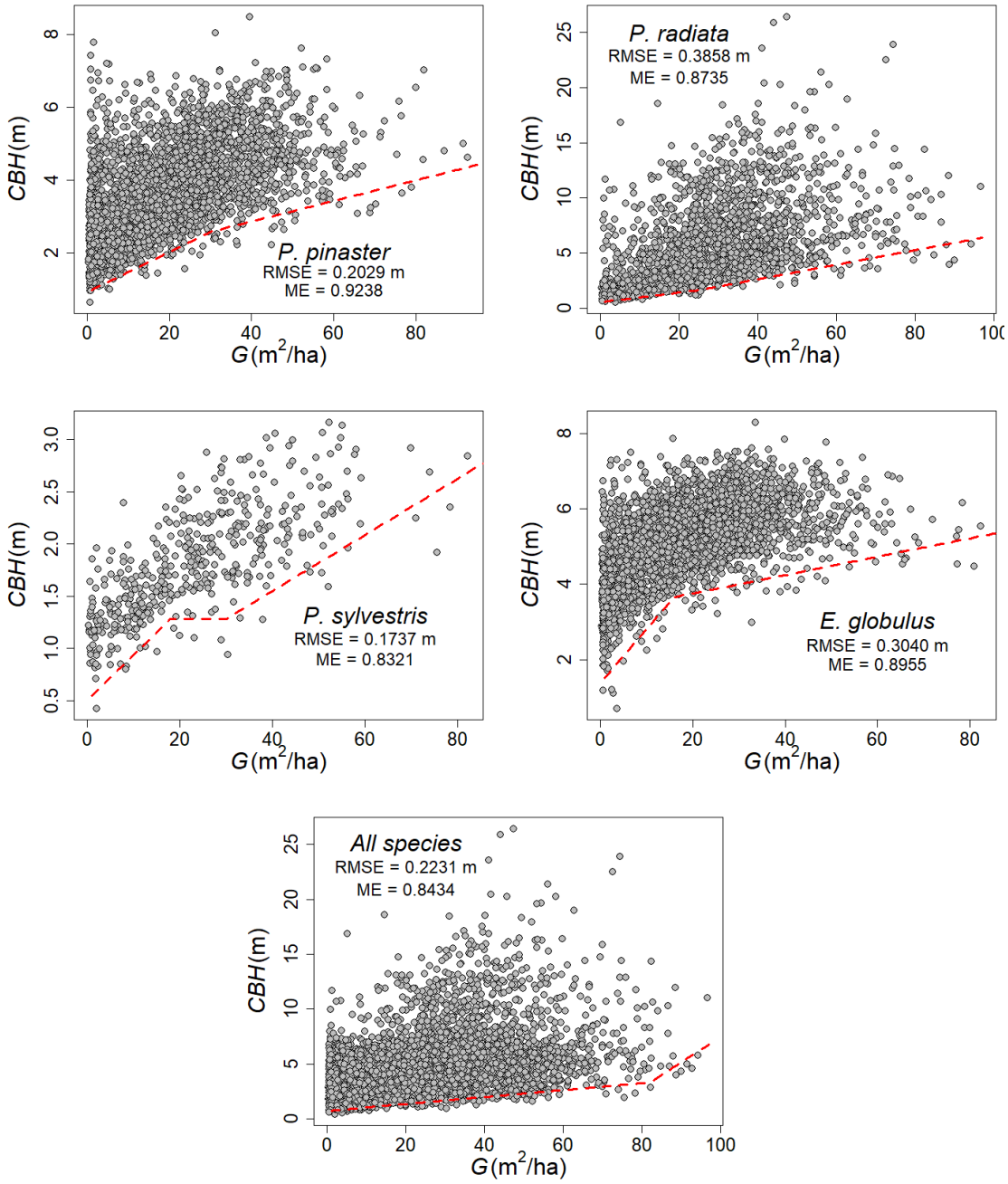

423 **Figure 2**. Plots of observed values of W_{shr_G1}, *CBH* and *CBD* versus stand basal area
424 (G) for each of the four overstorey species considered in this study and for all species
425 together. The red dashed line represents the extreme response MARS model fit.

426

427 *Dynamic models. Step 1: logistic models*

428 The mathematical expressions of the logistic models fitted to estimate the probability of
429 fire hazard increment (increment of W_{shr_G1} or *CBD* values) in the time interval Δt based

on current values of the variable of interest ($W_{shr\_G1\_1}$ or CBD_1, respectively) and a stand density proxy for each of the four tree species considered and for all species together are shown in Table 3.

Table 3. Mathematical expression and statistical measures of performance of the logistic models for estimating the probability that W_{shr_G1} and *CBD* will increase in the time interval Δt (years) based on current values of the variable of interest ($W_{shr\_G1\_1}$ or CBD_1, respectively) and a stand density proxy for each of the four tree species considered and for all species together.

Probability of increase in fine shrub fuel load ($W_{shr\ G1}$)	
Species	**Equation**
P. pinaster	$p = \left[\frac{\exp(3.7340 - 0.6301\ CC_1 - 0.8985\ W_{shr\_G1\_1})}{1 + \exp(3.7340 - 0.6301\ CC_1 - 0.8985\ W_{shr_{G1\_1}})}\right]^{\Delta t}$ Concordant pairs = 73.21%. Threshold (p = 0.51) (Sensitivity = 67.83%; Specificity = 67.21%; Accuracy = 67.50%)
P. radiata	$p = \left[\frac{\exp(3.7376 - 0.6137\ CC_1 - 1.0057\ W_{shr\_G1\_1})}{1 + \exp(3.7376 - 0.6137\ CC_1 - 1.0057\ W_{shr\_G1\_1})}\right]^{\Delta t}$ Concordant pairs = 72.94%. Threshold (p = 0.56) (Sensitivity = 68.86%; Specificity = 66.67%; Accuracy = 67.76%)
P. sylvestris	$p = \left[\frac{\exp(3.8033 - 0.4913\ CC_1 - 0.9063\ W_{shr\_G1\_1})}{1 + \exp(3.8033 - 0.4913\ CC_1 - 0.9063\ W_{shr\_G1\_1})}\right]^{\Delta t}$ Concordant pairs = 73.01%. Threshold (p = 0.45) (Sensitivity = 68.52%; Specificity = 65.387%; Accuracy = 66.67%)
E. globulus	$p = \left[\frac{\exp(3.9650 - 0.3910\ CC_1 - 1.0513\ W_{shr_{G1\_1}})}{1 + \exp(3.9650 - 0.3910\ CC_1 - 1.0513\ W_{shr\_G1\_1})}\right]^{\Delta t}$ Concordant pairs = 73.36%. Threshold (p = 0.43) (Sensitivity = 76.49%; Specificity = 58.53%; Accuracy = 67.96%)
All species	$p = \left[\frac{\exp(3.8312 - 0.5686\ CC_1 - 0.9776\ W_{shr_{G1\_1}})}{1 + \exp(3.8312 - 0.5686\ CC_1 - 0.9776\ W_{shr\_G1\_1})}\right]^{\Delta t}$ Concordant pairs = 72.86%. Threshold (p = 0.53) (Sensitivity = 69.24%; Specificity = 65.16%; Accuracy = 67.14%)
Probability of increase in canopy bulk density (*CBD*)	
Species	**Equation**
P. pinaster	$p = \left[\frac{\exp(4.9026 - 11.6799\ CBD_1)}{1 + \exp(4.9026 - 11.6799\ CBD_1)}\right]^{1/\Delta t}$ Concordant pairs = 76.21%. Threshold (p = 0.56) (Sensitivity = 89.27%; Specificity = 43.55%; Accuracy = 76.77%)

P. radiata	$p = \left[\frac{\exp(4.4065 - 9.0972\ CBD_1)}{1 + \exp(4.4065 - 9.0972\ CBD_1)}\right]^{1/\Delta t}$ Concordant pairs = 60.15%. Threshold (p = 0.62) (Sensitivity = 96.82%; Specificity = 7.59%; Accuracy = 81.36%)
P. sylvestris	$p = \left[\frac{\exp(4.9818 - 11.8918\ CBD_1)}{1 + \exp(4.9818 - 11.8918\ CBD_1)}\right]^{1/\Delta t}$ Concordant pairs = 83.49%. Threshold (p = 0.56) (Sensitivity = 83.12%; Specificity = 70.91%; Accuracy = 78.03%)
E. globulus	$p = \left[\frac{\exp(5.3380 - 0.0270\ CC_1 - 14.0987\ CBD_1)}{1 + \exp(5.3380 - 0.0270\ CC_1 - 14.0987\ CBD_1)}\right]^{1/\Delta t}$ Concordant pairs = 77.72%. Threshold (p = 0.63) (Sensitivity = 96.93%; Specificity = 20.69%; Accuracy = 84.71%)
All species	$p = \left[\frac{\exp(4.9550 - 0.4922\ CC_1 - 9.2701\ CBD_1)}{1 + \exp(4.9550 - 0.4922\ CC_1 - 9.2701\ CBD_1)}\right]^{1/\Delta t}$ Concordant pairs = 75.66%. Threshold (p = 0.57) (Sensitivity = 94.66%; Specificity = 31.70%; Accuracy = 80.51%)

The value of concordant pairs was around 73% in the five logistic models fitted for W_{shr_G1} but varied depending on the species for the *CBD* models, ranging from 60% for *P. radiata* to 83% for *P. sylvestris* (76% for all the species together). The logistic *CBD* models were more accurate than the W_{shr_G1} models, with sensitivity varying between 83% for *P. sylvestris* and 97% for *P. radiata* and *E. globulus*. Moreover, in these models, stand density, characterized by the initial values of *N*, *SDI*, *CC* or *G* was not significant for any of the species, except *E. globulus* and all species together, while in the shrub fine fuel load models, density, characterized by the current canopy cover (CC_1), was always significant.

Dynamic models. Step 2: transition functions

The mathematical expressions of the transition functions fitted to estimate the rate change of W_{shr_G1}, *CBH* and *CBD* during the time interval Δt (years) based on current values of the variable of interest ($W_{shr\_G1\_1}$, CBD_1 or CBH_1, respectively) and a stand density proxy for each of the four species analyzed and for all species together are shown in Table 4. All parameters were significant (α = 0.05), and graphical inspection

of the studentized residuals showed random patterns of residuals around zero with homogeneous variance and no discernible trends.

Table 4. Mathematical expression and goodness-of-fit statistics of the transition functions used to estimate the change of W_{shr_G1}, *CBH* and *CBD* during the time interval Δt (years) based on current values of the variable of interest ($W_{shr\_G1\_1}$, CBD_1 or CBH_1, respectively) and a stand density proxy for each of the four tree species considered and for all species together.

Fine shrub fuel load (W_{shr_G1}, kg/m^2) transition function	
Species	**Equation**
P. pinaster	$Y_2 = (5.42 - 2.03CC_1)\left(1 - \left[1 - \left[\frac{Y_1}{5.42 - 2.03CC_1}\right]^{0.89}\right]\exp^{-0.014\,\Delta t}\right)^{1.13}$ ME = 0.6364 RMSE = 0.4231 kg/m^2
P. radiata	$Y_2 = 2.95\left(1 - \left[1 - \left[\frac{Y_1}{2.95}\right]^{0.41}\right]\exp^{-0.055\,\Delta t}\right)^{2.43}$ ME = 0.5531 RMSE = 0.4955 kg/m^2
P. sylvestris	$Y_2 = (4.003 - 1.001CC_1)\left(1 - \left[1 - \left[\frac{Y_1}{4.003 - 1.001CC_1}\right]^{0.44}\right]\exp^{-0.026\,\Delta t}\right)^{2.26}$ ME = 0.8201 RMSE = 0.3348 kg/m^2
E. globulus	$Y_2 = (4.36 - 1.44CC_1)\left(1 - \left[1 - \left[\frac{Y_1}{4.36 - 1.44CC_1}\right]^{0.45}\right]\exp^{-0.034\,\Delta t}\right)^{2.21}$ ME = 0.5229 RMSE = 0.5311 kg/m^2
All species	$Y_2 = (3.26 - 0.69CC_1)\left(1 - \left[1 - \left[\frac{Y_1}{3.26 - 0.69CC_1}\right]^{0.34}\right]\exp^{-0.045\,\Delta t}\right)^{2.96}$ ME = 0.5717 RMSE = 0.4826 kg/m^2
Canopy bulk density (*CBD*, kg/m^3) transition function	
Species	**Equation**
P. pinaster	$Y_2 = (0.104 + 0.0404CC_1)\left(1 - \left[1 - \left[\frac{Y_1}{0.104 + 0.0404CC_1}\right]^{0.57}\right]\exp^{-0.063\,\Delta t}\right)^{1.76}$ ME = 0.5771 RMSE = 0.0218 kg/m^3
P. radiata	$Y_2 = 0.38\left(1 - \left[1 - \left[\frac{Y_1}{0.38}\right]^{0.83}\right]\exp^{-0.0088\,\Delta t}\right)^{1.21}$ ME = 0.8105 RMSE = 0.0152 kg/m^3
P. sylvestris	$Y_2 = 0.28\left(1 - \left[1 - \left[\frac{Y_1}{0.28}\right]^{0.78}\right]\exp^{-0.025\,\Delta t}\right)^{1.29}$ ME = 0.5712 RMSE = 0.0394 kg/m^3

E. globulus	$Y_2 = (0.11 + 0.039CC_1)\left(1 - \left[1 - \left[\frac{Y_1}{0.11 + 0.039CC_1}\right]^{0.68}\right]\exp^{-0.053\,\Delta t}\right)^{1.48}$ ME = 0.6006 RMSE = 0.0211 kg/m^3
All species	$Y_2 = 0.24\left(1 - \left[1 - \left[\frac{Y_1}{0.24}\right]^{0.97}\right]\exp^{-0.017\,\Delta t}\right)^{1.03}$ ME = 0.6626 RMSE = 0.0212 kg/m^3

Canopy base height (*CBH*, m) transition function

Species	Equation
P. pinaster	$Y_2 = (7.005 + 0.57CC_1)\left(1 - \left[1 - \left[\frac{Y_1}{7.005 + 0.57CC_1}\right]^{0.94}\right]\exp^{-0.030\,\Delta t}\right)^{1.06}$ ME = 0.7555 RMSE = 0.7351 m
P. radiata	$Y_2 = 59.53\left(1 - \left[1 - \left[\frac{Y_1}{59.53}\right]^{0.54}\right]\exp^{-0.010\,\Delta t}\right)^{1.85}$ ME = 0.8639 RMSE = 1.1351 m
P. sylvestris	$Y_2 = (2.65 + 0.54CC_1)\left(1 - \left[1 - \left[\frac{Y_1}{2.65 + 0.54CC_1}\right]^{0.92}\right]\exp^{-0.025\,\Delta t}\right)^{1.09}$ ME = 0.8121 RMSE = 0.4641 m
E. globulus	$Y_2 = 6.67\left(1 - \left[1 - \left[\frac{Y_1}{6.67}\right]^{0.96}\right]\exp^{-0.074\,\Delta t}\right)^{1.04}$ ME = 0.3104 RMSE = 0.8263 m
All species	$Y_2 = 9.29\left(1 - \left[1 - \left[\frac{Y_1}{9.29}\right]^{0.73}\right]\exp^{-0.019\,\Delta t}\right)^{1.37}$ ME = 0.7526 RMSE = 1.1004 m

4. DISCUSSION

4.1. Data characterization

The fuel loads of total understorey vegetation (W_{shr}) and fine understorey vegetation (W_{shr_G1}) estimated in this study are within the range observed by other authors under site conditions characterized by similar climatic, physiographical and edaphic conditions (e.g. González-Hernández et al., 1998; Vega, 2001; Fernandes et al., 2002, 2009; Fernandes and Rigolot, 2007; Cruz et al., 2011; Castedo-Dorado et al., 2012; Botequim et al., 2015; Arellano et al., 2017; Vega 2022a).

473 Regarding canopy variables, the mean *CBD* values are similar to those reported by
474 Nunes et al. (2022) for *P. pinaster*, *P. sylvestris* and *Eucalyptus* spp., estimated using
475 data from National Forest Inventories in Portugal and Spain, but lower than those
476 reported by Fernández-Alonso et al. (2013) for *P. pinaster*, *P. radiata and P. sylvestris*
477 stands in Galicia and estimated using SNFI-4 data. These discrepancies are probably
478 due to the much wider geographical and temporal scope of the present study, with
479 greater variability in site qualities and silvicultural treatments resulting in e.g. a wider
480 range of canopy lengths that affect *CBD* values. Mean canopy lengths were 45% higher
481 for *P. pinaster* and *P. radiata* and 35% higher for *P. sylvestris* in this study than those
482 reported by Fernandez-Alonso et al. (2013).

483 **4.2. Extreme response models**

484 A noticeable limit at maximum levels of the response variables is indicated by the
485 analysis of the two-dimensional plots of both W_{shr_G1} and *CBD* relative to *G* (Figure 2).
486 The same rationale applies to the minimum levels of *CBH*. These distributions suggest
487 that fuel complex characteristics in these commercial plantations are strongly limited by
488 overstorey stand density, expressed in terms of stand basal area (*G*).
489 These results suggest that the maximum fine shrub fuel loads that can be accumulated
490 by certain overstorey species depend on the availability of site resources (light, water,
491 nutrients). In a region such as the study area where rainfall is not usually highly
492 limiting, competition for light, which is closely linked to stand density (e.g. Wagner et
493 al., 2011; Valladares et al., 2016; Balandier et al., 2022), can be assumed to be a major
494 driver of understorey development. Data points in the interior of these distributions
495 indicate that shrub development is reduced by environmental factors (e.g. climate) or by
496 the management history of the plots (shrubby vegetation clearing, past wildfires, etc.)
497 (Suchar and Crookston, 2010; Botequim et al., 2015; Johnson et al., 2017; Landuyt et

al., 2019). The management history is particularly important in commercial plantations in northern Spain, where the establishment and development of shrubby vegetation are strongly affected by human activities (e.g. shrub clearing when trees are planted or during the rotation cycle) (e.g. Tomé et al., 2021; Rodríguez-Soalleiro and Madrigal, 2008). In addition, even when the same amount of light is transmitted by the overstorey, development of the understorey can vary substantially between shrub species (e.g. Gaudio et al., 2008; Balandier et al., 2022). Moreover, the understorey communities in the present study varied widely below the same dominant overstorey tree species, and therefore the points in the interior of the distribution may also reflect the diversity of light requirements by shrub communities.

The highest predicted values of W_{shr_G1} according to the extreme response models (99th percentile) were obtained for *P. pinaster* and *E. globulus* when *G* is close to zero, which usually corresponds with the early stages of stand development. At these stages, trees and shrubs engage in a balanced competition, resulting in understorey loads that closely resemble those found in treeless shrublands within the same ecosystem (Arellano et al., 2017; Vega et al., 2022a). Shrub clearing and land preparation for tree planting produce perturbed areas prone to being colonized by generalist and shade-intolerant species such as those of the genera *Erica* and *Ulex*. The biomass of these species can increase greatly after disturbance, due to the high resprouting capacity (Fernández et al., 2013; Montero et al., 2020).

Interestingly, there seems to be an initial range of stand basal area below which the decline in W_{shr_G1} load is slight, and above which it is more pronounced. This threshold is species-specific, varying between 20 m^2/ha for *P. sylvestris*, 50 m^2/ha for *E. globulus* and 40 m^2/ha for *P. pinaster*. Additionally, an extinction point for the fine shrub fuel load can be inferred for these three species, corresponding to a value of 80 m^2/ha for *P.*

sylvestris, and reaching *circa* 100 m^2/ha for *E. globulus* and *P. pinaster.* The former segment can roughly define the period when shrubs reach their adult size, and biomass tends to stabilize, whereas the latter defines the senescence period of shrubby plants, mainly mediated by light availability. The eucalyptus stands can sustain a shrub fuel load higher than 2.2 kg/m^2 at a higher *G* (50 m^2/ha) than pine species (except for *P. radiata*), which is probably due to the particular crown architecture of blue gum trees, in which canopy cover (LAI) is relatively smaller for similar *G* (e.g. Sands and Landsberg, 2002; Bakker et al., 2009; Lopes et al., 2016).

The difference in performance of *P. sylvestris* and the other two species may be related to the comparatively lower light transmittance in *P. sylvestris* (Silva-Pando et al., 2002; Balandier et al., 2022) than in *P. pinaster* (Gonzalez et al., 2013; Balandier et al., 2022) and *E. globulus* (Ruiz et al., 2008). A slightly different pattern emerged for *P. radiata*, with W_{shr_G1} above 2 kg/m^2 constrained for the entire range of *G* considered, suggesting that the maximum shrub fuel load for this tree species is less dependent on the stand density. Although confirming previous findings (Castedo-Dorado et al., 2012; Vega et al., 2022a), this result apparently contradicts the lower light transmission in stands of this species, at least in comparison with that of *P. pinaster* (Castedo-Dorado et al., 2011). In radiata pine stands, the understorey communities can be dominated by species that take advantage of fresh soil moisture conditions (Onaindia et al., 2013). Some of these species can develop even under the low levels of light transmitted through the overstorey to the understorey (Gaudio et al., 2008; Harmer et al., 2012; Balandier et al., 2022), which could explain the low sensitivity of the fine shrub fuel load to variations in stand density. In addition, *P. radiata* is frequently planted in former agricultural and pasture lands (Pérez-Cruzado, 2011), where availability of soil and nutrients can enhance shrub development.

548 A tendency for the variables that describe the canopy fuel layer (*CBD* and *CBH*) to
549 increase with increasing *G* can be seen in the two-dimensional plots (Figure 2),
550 particularly in the case of *CBD*. This latter result is expected as *G* is a measure of stand
551 occupancy, which results in denser stands with a large amount of canopy biomass. This
552 supports previous reports indicating that *G* is the most important variable correlated
553 with available canopy fuel (Cruz et al., 2003; Gómez-Vázquez et al., 2013; Fernández-
554 Alonso et al., 2013; Mitsopoulos and Dimitrakopoulos, 2014; Mitsopoulos and
555 Xanthopoulos, 2016). For all species except *P. sylvestris*, the extreme response models
556 relate the *CBD* and *G* in a general linear relationship. For *P. sylvestris*, the trend is not
557 as clear, probably due to the scarcity of observations for stands of this species, with *G*
558 values greater than 40 m^2/ha and the large variability in the limited observations (Figure
559 2).
560 The minimum response models for *CBH* describe the tendency for the 1st percentile of
561 this variable to be linearly related to *G* in *P. radiata* and *P. pinaster,* whereas in *P.*
562 *sylvestris* and *E. globulus*, the relationship is not linear. A steeper regression slope may
563 be expected for maritime pine stands than for radiata pine stands, because maritime pine
564 ranks intermediate in a scale of self-pruning (Keeley and Zedler, 1998), whereas radiata
565 pine is characterised by very poor self-pruning, even in limited light-conditions (e.g.
566 Alonso-Rego et al., 2022). For stands dominated by *E. globulus*, *CBH* increases rapidly,
567 but the slope moderates when *G* is greater than *circa* 20 m^2/ha. This trend can be
568 attributed to more active self-pruning at younger ages (Mirra et al., 2017).
569 Adequate results were obtained by modelling minimum *CBH* with *G* as a regressor. In
570 mean response models, *CBH* is usually highly correlated with stand height, because the
571 base of the canopy moves vertically along the stem as stand height increases (Cruz et
572 al., 2003). Stand density therefore usually has little influence on *CBH* development

(Fernández-Alonso et al., 2013; Gómez-Vázquez et al., 2013). Overall, our results suggest that stand density may modulate the minimum values of *CBH* reached in a plot for a certain stand height.

Basal area has previously been found to be a limiting factor in understorey fuel load, in both mean response models (e.g. Kerns and Ohmann, 2004; Botequeim et al., 2015; Mitsopoulos and Xanthopoulos, 2016; Vega et al., 2022a) and extreme response models (Coll et al., 2011; Castedo-Dorado et al., 2012; Russell et al., 2014; Mitsopoulos and Xanthopoulos, 2016). Some authors have found that other measures of stand density such as the stand density index (McKenzie et al., 2000), relative spacing index (Fonseca and Duarte, 2017) and canopy cover (Knowles et al., 1999; Cole et al., 2010) were better stand predictors than *G*; however, this was not the case with our experimental data. *G* can be considered a proxy for the overstorey leaf area index (Balandier et al., 2022), and also a surrogate for the relative availability of nutrients or water in the soil. Basal area has the additional advantage that future projection from growth and yield models is relatively simple (see Diéguez-Aranda et al., 2009 and García Villabrille, 2015 for pine species and blue gum, respectively, in northern Spain).

The extreme response models developed here have a relatively high predictive capacity, especially for canopy fuel characteristics. The poorer predictions regarding shrub fine fuel load understorey add evidence to the inherent difficulty in making predictions about understorey vegetation characteristics (Suchar and Crookston, 2010; Coll et al., 2011; Russell et al., 2014; Botequim et al., 2015; Sánchez-Pinillos et al. 2021).

4.3. Dynamic models

The present research extends the two previous studies on the dynamics of fuel complex variables in the study region (Ruiz-González et al., 2015; Botequim et al., 2015) in different ways. First, the two-step regression approach used allows more realistic

598 modelling of the dynamics of the fuel complex associated with both stand growth and
599 the potential modulation effects of stand density. Thus, the probability that W_{shr_G1} and
600 *CBD* will increase can be predicted using logistic equations, and if the value falls below
601 a certain threshold, a decrease in the shrub fuel biomass or in *CBD* can be expected to
602 occur. The negative sign of the parameter estimates for the current values of these
603 variables ($W_{shr\_G1\_1}$ and CBD_1) seems realistic, because the levels suggest that the
604 probability of an increase in the values will decrease when the current values are large.
605 The same rationale applies to the negative sign of the parameters estimates for the
606 current overstorey canopy cover (CC_1) in the fine shrub biomass equation, indicating
607 that decrease in the latter variable is more likely when the overstorey competition
608 increases.
609 In the second step, the transition functions enable the future values of W_{shr_G1}, *CBD* and
610 *CBH* to be estimated on the basis of an initial known quantity of these variables, the
611 projection length (Δt, years), and, for some species, the current overstorey canopy cover
612 (CC_1). Note that in developing the transition functions we only considered the plots in
613 which a change in fire-related variables towards higher fire hazard conditions between
614 inventories was estimated in the first step by the logistic equations. This helps to explain
615 why the initial value of the dependent variables ($W_{shr\_G1\_1}$, CBD_1 and CBH_1) in this
616 system of equations has a positive effect on the projected value. Additionally, the sign
617 of the parameter estimates corresponding to initial canopy cover (CC_1) seems realistic:
618 negative for W_{shr_G1} transition functions and positive for *CBH* and *CBD* transition
619 functions. This implies that, if the remaining explanatory variables are equal, for larger
620 current canopy cover, the increase in W_{shr_G1} will be smaller and the increase in *CBD*
621 and *CBH* will be larger.

622 The dynamic models developed here are age-independent and they are therefore more
623 useful for practical applications. Moreover, if information on initial shrub biomass is
624 not available, the fuel load models from area-based shrub metrics developed here (see
625 Supplementary material) can be used for initialization. The initial values of the
626 remaining overstorey variables (*CC*, *CBH* and *CBD*) can be easily calculated from data
627 obtained from a common forest inventory in which both *dbh* and *h* are measured.
628 An additional valuable characteristic of the dynamic models developed here is that they
629 were constructed using data from a national forest inventory, which thus cover a wide
630 spatio-temporal scale. The plots considered cover the most common combinations of
631 stand ages, stand densities and sites for major commercial plantations in northern Spain,
632 which extends the applicability of the developed models to most of the wooded area in
633 the region. This is considered an advantage relative to site-specific models, which have
634 limited extrapolation capacity. We also assessed the variation in fuel complex
635 characteristics throughout the period covered by the SNFI in northern Spain. Thus, for
636 comparable plots, the time interval between SNF2 and SNFI4 is 30 years (1997-2018).
637 Although for many plots the time interval between inventories is shorter, it is
638 considered long enough to describe the dynamics of the fuel complex in the medium
639 and long term (Sánchez-Pinillos et al., 2021).

640 **4.4. Limitations of the extreme and dynamic models**

641 Several limitations of the proposed models can also be highlighted. First, the model
642 developed for estimating fine shrub fuel load was fitted using data obtained from
643 destructively sampled plots dominated by the three pine species and was not only
644 applied to pine-dominated plots but also to eucalyptus-dominated plots. Although
645 previous studies in the study region (Botequim et al., 2015) found that forest
646 composition does not contribute significantly to explaining the variation in shrub

biomass, some differences can be expected because of the different interception in light according to the architectural structure of the tree (Balandier et al, 2022). Based on these differences, some authors state that certain shrub species display a special affinity for a particular overstorey type (Bartels and Chen, 2010; Bonari et al., 2017). Nevertheless, such affinity refers to native forest stands. By contrast, the plantations under study here were established on previous treeless shrubland communities without any apparent association with the tree species established. Moreover, an understorey species that often dominates the plantation understorey in high quality sites (the bracken fern *Pteridium aquilinum* (L.) Kuhn in Kerst.) was not evaluated in the SNFI surveys. However, the implication for fire risk is expected to be minor, as the mean values of total fuel loads for this species represents less than 30% of the mean values of W_{shr} in understorey shrub formations in the stands of the three pines (Vega et al., 2022a) and, in addition, their peak flammability occurs in autumn (Fernandes and Rigolot, 2007). Second, only the fuel layers corresponding to understorey vegetation and canopy were considered here; other main components of the fuel complex such as forest floor or some ladder fuels, especially suspended needles and twigs in the lower canopy, which can be important in maritime pine and radiata pine stands (Fernandes and Rigolot, 2007; Alonso-Rego et al., 2022), were not considered. In highly stocked stands, ladder fuels may contribute substantial amounts of fuel, thus significantly increasing the risk of crown fire (de Ronde et al., 1990; Cruz et al., 2017). Nevertheless, the SNFI does not provide data on this type of fuels, and estimation via stand variables is not straightforward. Regarding the forest floor, although the SNFI provides a combined assessment of the depth of soil organic layers, i.e. L (fresh litter), F (partially decomposed litter) and H (raw humus), the level of detail of these data source is not sufficient for robust modelling (López-Senespleda et al., 2021). The forest floor is

672 critical in fire management due to its flammability in a broad sense (Burton et al.,
673 2021), as well as the central role played in soil burn severity generation through
674 smouldering combustion (Vega et al., 2013). Litter and fine woody debris can account
675 for 33% (Vega et al., 2022a), 52% (Arellano et al., 2017) or 64% (Arellano et al., 2020)
676 of the average fuel load of *G*1 (<6 mm) in the forest stands in the region, representing a
677 significant proportion of the fuel hazard.
678 Although speculatively, it can be hypothesized that models describing the extreme
679 distribution and temporal dynamics of forest floor in the study area will also depend on
680 some stand density proxy. Thus, previous research on pine forests in the region (Vega et
681 al., 2022b) revealed a significant relationship between total litter and duff load and the
682 overstorey basal area in a mean response model. In addition, Fernandes et al. (2002)
683 developed a litter load model for *P. pinaster* as a function of basal area and stand age, in
684 an adjacent region of the Iberian Peninsula.
685 Third, although plots with explicit signs of recent human activity in the understorey
686 (e.g. bush clearing) were excluded from analysis, we have no detailed information on
687 previous disturbance, which was found to be an important variable for predicting
688 surface fuel loads in other regions (e.g. Parresol et al., 2012; Botequim et al., 2015). In
689 addition, the history of the use of the plots prior to plantation establishment is not
690 known. In this way, human pressure has been exerted over millennia throughout the
691 region, including periodic burning, slashing, grazing and temporary cultivation (e.g.
692 Valbuena-Carabaña et al., 2010), probably relative uniformly in most plots.
693 Finally, our modelling approach focused only on including the effect of stand density on
694 the equations developed. The inclusion of other factors such as physiographic, edaphic
695 and climatic variables (Suchar and Crookston, 2010; Botequim et al., 2015; Sánchez-
696 Pinillos et al., 2021) would probably improve the accuracy of the estimates, although

hindering practical use of the models. This question should be considered in future research.

4.5. Conclusions and implications for fuel hazard and fire management

Although the understorey has an important impact on fire risk, with obvious implications for fire and forest planning in commercial plantations (e.g. Botequim et al., 2013; Nunes et al., 2019), modelling the understorey biomass and the effects of overstorey on understorey biomass has received less attention (Fernandes et al., 2002, 2009; Castedo-Dorado et al., 2012; Botequim et al., 2015; Vega et al., 2022a).

The models developed here add knowledge to this subject in different ways. We developed robust models for estimating understorey fuel loads from area-based understorey metrics. These models can be generalized to the stands where one of the four tree species considered dominate the overstorey. These models can also be used to estimate shrub fuel accumulation at a specific point in time, and to initialize the value in the dynamic $Wshr_{\_G1}$ model.

The extreme response models quantify the maximum shrub fine fuel biomass and *CBD* and the minimum *CBH* that a stand dominated by one of the four overstorey species can sustain for a specific value of overstorey density. Therefore, these models can be used as the basis for worst-case-scenarios in wildfire simulations to characterize the potential fire behaviour in a given stand (Suchar and Crookston, 2010), as well as to assess the thresholds at which *G* could constrain fire behaviour.

One example of the direct implication of these extreme response models in fuel hazard assessment involves planting density. The silviculture of commercial species in northern Spain (particularly pines) usually includes establishing high initial densities to control shrub fuel development and to prevent high intensity surface fires and crowning (Crecente-Campo et al., 2009; Serrada et al., 2011). The presents findings suggest that

722 this overstorey management does not prevent shrub growth, at least in young (low *G*)
723 stands, and that a very high *G* would be necessary for early effective control of the
724 understorey vegetation. Moreover, these high *G* values may be associated with high
725 *CBD* values. Thus, according to the extreme response models fitted here, the threshold
726 of 0.1 kg/m^3 empirically deduced by Agee (1996) as the approximate value necessary to
727 support active crowning can be exceeded for *G* greater than 20 m^2/ha.
728 Our findings also suggest that both the shrub and canopy layers are responsive to stand
729 density management practices through thinning, and that these practices can result in
730 trade-offs between the three fuel complex variables analysed. This is especially
731 important for pine species where managed-induced changes in *G* (usually, 1 to 3
732 thinning from below are carried out up to the rotation age) occur. With the aim of
733 reducing fire risk, forest managers must find a balance between decreasing canopy bulk
734 density and maintaining shrub fuel loads.
735 The dynamic models allow estimation of whether fire hazard will increase in the future
736 owing to an increase in the fuel complex characteristics W_{shr_G1} and *CBD*. If the values
737 of these fuel complex variables increase, the future values can be estimated from the
738 current values and the overstorey canopy cover.
739 The surface fire behaviour and its subsequent transition to the canopy and propagation
740 as a crown fire depends on topographic, meteorological, fuel structure and fuel moisture
741 factors. Among the fuel structural variables, W_{shr_G1}, *CBH* and *CBD* are common
742 explanatory variables in wildfire behaviour simulations (Alexander and Cruz, 2016).
743 Assessment of the likelihood of fire initiation and the rate of spread of crown fires is
744 recommended prior to the implementation of fuel management programmes aimed at
745 mitigating the occurrence of high-intensity fires. Accordingly, the models developed
746 here can be useful to support optimal forest management decisions (e.g. Piqué et al.,

2022). Specifically, they enable proposal of better-suited density prescriptions to the overstorey tree species in order to minimize both the probability of crown fire initiation (related to the fine fuel load of understorey vegetation and the height where *CBH* occurs) and spread (related to the bulk density of canopy fuels, *CBD*). This strategic adaptive measure would assist in reducing the vulnerability of commercial plantations to wildfire.

5. FUNDING SOURCES

This work was supported by the project INIA-RTA2017-00042-C05 (VIS4FIRE) of the Spanish National Program of Research, Development and Innovation cofunded by the ERDF Program of the European Union, and by Programa Estatal de I+D+i 2017-2020 proyectos orientados a los Retos de la Sociedad, RTA. Agencia Estatal de Investigación, INIA [grant number PID2020-116494RR-C42: Mejora de la resiliencia a los incendios de los sistemas forestales mediterráneos (NO de España) ENFIRES-NO].

6. REFERENCES

Agee, J.K., 1996. The influence of forest structure on fire behavior, in: Cooper, S.L. (Ed.), Proceedings of the 17th annual forest vegetation management conference. Redding, CA., pp. 52-68.

Agee, J.K., Skinner, C.N., 2005. Basic principles of forest fuel reduction treatments. For. Ecol. Manage. 211, 83–96. https://doi.org/10.1016/j.foreco.2005.01.034

Aguirre, A., Moreno-Fernández, D., Alberdi, I., Hernández, L., Adame, P., Cañellas, I., Montes, F., 2022. Mapping forest site quality at national level. For. Ecol. Manage. 508, 120043. https://doi.org/10.1016/j.foreco.2022.120043

771 Alberdi Asensio, I., Condés Ruiz, S., Martínez Millán, J., Saura Martínez de Toda, S.,
772 Sánchez Peña, G., Pérez Martín, F., Villanueva Aranguren, J.A., Vallejo Bombin,
773 R., 2010. Spanish National Forest Inventory, in: Tomppo, E., Gschwantner, T.,
774 Lawrence, M., McRoberts, R.E., (Eds.). National Forest Inventories. Pathways for
775 Common Reporting. Springer, pp. 527-540.
776 Alberdi, I., Vallejo Bombín, R., Álvarez-González, J.G., Condes Ruiz, S., González
777 Ferreiro, E., Guerrero García, S., Hernández Mateo, L., Martínez Jaúregui, M.,
778 Monte, F., de Oliveira Rodríguez, N., Pasalodos Tato, M., Robla, E., Ruiz
779 González, A.D., Sánchez González, M., Sandoval, V., San Miguel Ayanz, A., Sixto
780 Blanco, H., Cañellas, I., 2017. The multi-objective Spanish national forest
781 inventory. For. Syst. 26, 14. https://doi.org/10.5424/fs/2017262-10577
782 Alexander, M.E., Cruz, M.G., 2011. Crown fire dynamics in conifer forests, in: Werth,
783 P.A., Potter, B.E., Clements, C.B., Finney, M.A., Goodrick, S.C., Alexander, M.E.,
784 Cruz, M.G., Forthofer, J.A., McAllister, S.S. (Eds.), Synthesis of Knowledge of
785 Extreme Fire Behavior, Volume I for Fire Managers. Gen. Tech. Rep. PNW-GTR-
786 854, Portland, pp. 107–142.
787 Alexander, M.E., Cruz, M.G., 2016. Crown Fire Dynamics in Conifer Forests, in:
788 Werth, P.A., Potter, B.E., Alexander, M.E., Clements, C.B., Cruz, M.G., Finney,
789 M.A., Jason M. Forthofer, J.M., Goodrick, S.L., Hoffman, C., Jolly, W.M.,
790 McAllister, S.S., Ottmar, R.D., Parsons, R.A. (Eds.). Synthesis of knowledge of
791 extreme fire behavior: volume 2 for fire behavior specialists, researchers, and
792 meteorologists. USDA Forest Service Gen. Tech. Rep. PNW-GTR-891, Portland,
793 pp. 163-258.
794 Alonso-Rego, C., Fernandes, P., Álvarez-González, J.G., Arellano-Pérez, S., Ruiz-
795 González, A.D., 2022. Individual-tree and stand-level models for estimating ladder

796 fuel biomass fractions in unpruned *Pinus radiata* plantations. Forests 13, 1697.
797 https://doi.org/10.3390/f13101697
798 Ameztegui, A., Coll, L., 2013. Unraveling the role of light and biotic interactions on
799 seedling performance of four Pyrenean species under environmental gradients. For.
800 Ecol. Manage. 303, 25–34. https://doi.org/10.1016/j.foreco.2013.04.011
801 Arellano, S., Vega, J.A., Ruiz-González, A.D., Arellano, A., Álvarez-González, J.G.,
802 Vega, D.J., Pérez, E., 2017. Foto-guía de combustibles forestales de Galicia y
803 comportamiento del fuego asociado. Andavira, Santiago de Compostela, Spain.
804 Arellano-Pérez, S., Castedo-Dorado, F., Álvarez-González, J.G., Alonso-Rego, C.,
805 Vega, J.A., Ruiz-González, A.D., 2020. Mid-term effects of a thin-only treatment
806 on fuel complex, potential fire behaviour and severity and post-fire soil erosion
807 protection in fast-growing pine plantations. For. Ecol. Manage. 460, 117895.
808 https://doi.org/10.1016/j.foreco.2020.117895
809 Bakker, M.R., Jolicoeur, E., Trichet, P., Augusto, L., Plassard, C., Guinberteau, J.,
810 Loustau. D., 2009. Adaptation of fine roots to annual fertilization and irrigation in
811 a 13-year-old *Pinus pinaster* stand. Tree Physiol. 29, 229–238.
812 https://doi.org/10.1093/treephys/tpn020
813 Balandier, P., Mårell, A., Prévosto, B., Vincenot, V., 2022. Tamm review: Forest
814 understorey and overstorey interactions: So much more than just light interception
815 by trees. For. Ecol. Manage. 526, 120584.
816 https://doi.org/10.1016/j.foreco.2022.120584
817 Bartels, S.F., Chen, H.Y., 2010. Is understory plant species diversity driven by resource
818 quantity or resource heterogeneity? Ecology, 91, 1931-1938.
819 https://www.jstor.org/stable/25680443

820 Bertalanffy, L.v., 1957. Quantitative laws in metabolism and growth. Q. Rev. Biol. 32,
821 217–231. https://www.jstor.org/stable/2815257
822 Bilgili, E., 2003. Stand development and fire behavior. For. Ecol. Manage. 179, 333–
823 339. https://doi.org/10.1016/S0378-1127(02)00550-9
824 Bilgili, E., Methven, I.R., 1994. A dynamic fuel model for use in managed even-aged
825 stands. Int. J. Wildland Fire 4, l77–185. https://doi.org/10.1071/WF9940177
826 Bliss, C., 1938. The transformation of percentages for use in the analysis of variance.
827 Ohio J. Sci. 38, 9–12.
828 Bonari, G., Acosta, A.T., Angiolini, C., 2017. Mediterranean coastal pine forest stands:
829 understorey distinctiveness or not?. For. Ecol. Manage. 391, 19-28.
830 https://doi.org/10.1016/j.foreco.2017.02.002
831 Botequim, B., Garcia-Gonzalo, J., Marques, S., Ricardo, A., Borges, J.G., Tomé, M.,
832 Oliveira, M.M., 2013. Developing wildfire risk probability models for *Eucalyptus*
833 *globulus* stands in Portugal. iForest 6, 217-227. https://doi.org/10.3832/ifor0821-
834 006
835 Botequim, B., Zubizarreta-Gerendiain, A., Garcia-Gonzalo, J., Silva, A., Marques, S.,
836 Fernandes, P.M., Pereira, J.M.C., Tomé, M., 2015. A model of shrub biomass
837 accumulation as a tool to support management of Portuguese forests. iForest 8,
838 114-125. https://doi.org/10.3832/ifor0931-008
839 Burkhart, H.E., Tomé, M., 2012. Modeling Forest Trees and Stands. Springer Science &
840 Business Media. https://doi.org/10.1007/978-90-481-3170-9
841 Burton, J.E., Cawson, J.G., Filkov, A.I., Penman, T.D., 2021. Leaf traits predict global
842 patterns in the structure and flammability of forest litter beds. J. Ecol. 109, 1344–
843 1355. https://doi.org/10.1111/1365-2745.13561

Byram, G.M. 1959. Combustion of Forest Fuels, in: Davis, K.P. (Ed.), Forest fire: control and use. McGraw-Hill, New York.

Calkin, D.E., Ager, A.A., Gilbertson-Day, J., Scott, J., Finney, M., Schrader-Patton, C., Quigley, T., Strittholt, J., Kaiden, J., 2010. Wildfire Risk and Hazard: Procedures for the First Approximation. USDA Forest Service Gen Tech. Rep. RMRS-GTR-235, Fort Collins, CO, USA, 62p. https://doi.org/10.2737/RMRS-GTR-235

Castedo-Dorado, F., Faba-Fernández, M., Rodríguez-Pérez, J.R., 2011. Relaciones entre variables de rodal y variables obtenidas mediante fotografías hemisféricas en masas de *Pinus pinaster* y *Pinus radiata* en el noroeste de España, in: Recondo, C., Pendás, E. (Eds.), XIV Congreso de la Asociación Española de Teledetección, pp. 85-88.

Castedo-Dorado, F., Gómez-Vázquez, I., Fernandes, P.M., Crecente-Campo, F., 2012. Shrub fuel characteristics estimated from overstory variables in NW Spain pine stands. For. Ecol. Manage. 275, 130-141. https://doi.org/10.1016/j.foreco.2012.03.002

Chuvieco, E., Yebra, M., Martino, S., Thonicke, K., Gómez-Giménez, M., San-Miguel, J., Oom, D., Velea, R., Mouillot, F., Molina, J.R., Miranda, A., Lopes, D., Salis, M., Bugaric, M., Sofiev, M., Kadatnsev, E., Gitas, I.Z., Stavrakoudis, D., Eftychidis, G., Bar-Massada, A., Neidermeier, A., Pampanoni, V., Pettinari, M.L., Arrogante-Funes, F., Ochoa, C., Moreira, B., Viegas, D., 2023. Towards an integrated approach to wildfire risk assessment: when, where, what and how may the landscapes burn. Fire 6, 215. https://doi.org/10.3390/fire6050215

Cole, E.C., Hanley, T.A., Newton, M., 2010. Influence of precommercial thinning on understory vegetation of young-growth Sitka spruce forests in southeastern Alaska. Can. J. For. Res. 40, 619-628. https://doi.org/10.1139/X10-009

869 Coll, L., González-Olabarria, J.R., Mola-Yudego, B., Pukkala, T., Messier, C., 2011.
870 Predicting understory maximum shrubs cover using altitude and overstory basal
871 area in different Mediterranean forests. Eur. J. For. Res. 130, 55-65.
872 https://doi.org/10.1007/s10342-010-0395-y
873 Crecente-Campo, F., Pommerening, A., Rodríguez-Soalleiro, R., 2009. Impacts of
874 thinning on structure, growth and risk of crown fire in a *Pinus sylvestris* L.
875 plantation in northern Spain. For. Ecol. Manage. 257, 1945-1954.
876 https://doi.org/10.1016/j.foreco.2009.02.009
877 Cruz, M.G., Alexander, M.E., Fernandes, P.A.M., 2008. Development of a model
878 system to predict wildfire behaviour in pine plantations. Aust. For. 71, 113–121.
879 https://doi.org/10.1080/00049158.2008.10676278
880 Cruz, M.G., Alexander, M.E., Plucinski, M.P., 2017. The effect of silvicultural
881 treatments on fire behaviour potential in radiata pine plantations of South Australia.
882 For. Ecol. Manage. 397, 27–38. https://doi.org/10.1016/j.foreco.2017.04.028
883 Cruz, M.G., Alexander, M.E., Wakimoto, R.H., 2003. Assessing canopy fuel stratum
884 characteristics in crown fire prone fuel types of western North America. Int. J.
885 Wildland Fire 12, 39–50. https://doi.org/10.1071/WF12008_CO
886 Cruz, M.G., Alexander, M.E., Wakimoto, R.H., 2004. Modeling the likelihood of crown
887 fire occurrence in conifer forest stands. For. Sci. 50, 640-658.
888 https://doi.org/10.1093/forestscience/50.5.640
889 Cruz, M.G., Alexander, M.E., Wakimoto, R.H., 2005. Development and testing of
890 models for predicting crown fire rate of spread in conifer forest stands. Can. J. For.
891 Res. 35, 1626-1639. https://doi.org/10.1139/x05-085

892 Cruz, M.G., Butler, B.W., Alexander, M.E., Forthofer, J.M., Wakimoto, R.H., 2006.
893 Predicting the ignition of crown fuels above a spreading surface fire. Part I: model
894 idealization. Int. J. Wild. Fire 15, 47-60. https://doi.org/10.1071/WF04061
895 Cruz, M.G., de Mar, P.J., Adshead, D., 2011. Radiata pine plantation fuel and fire
896 behaviour guide. CSIRO and GHD publication for the Australian Government
897 Department of Agriculture, Fisheries and Forestry, Camberra, ACT, 23 pp.
898 da Silva, J.A.T., Karimi, J., Mohsenzadeh, S., Dobranszki, J., 2015. Allelopathic
899 potential of select gymnospermous trees. J. For. Environ. Sci. 31, 109-118.
900 http://dx.doi.org/10.7747/JFES.2015.31.2.109
901 De Cáceres, M., Casals, P., Gabriel, E., Castro, X., 2019. Scaling-up individual-level
902 allometric equations to predict stand-level fuel loading in Mediterranean
903 shrublands. Ann. For. Sci. 76, 87. https://doi.org/10.1007/s13595-019-0873-4
904 de Ronde, C., Goldammer, J.G., Wade, D., Soares, R.V., 1990. Prescribed fire in
905 industrial pine plantations, in: Goldammer, J. (Ed.), Fire in the Tropical Biota:
906 Ecosystem Processes and Global Challenges. Springer-Verlag, Berlin, pp. 216–272.
907 Del Grosso, S., Parton, W., Stohlgren, T., Zheng, D., Bachelet, D., Prince, S., Hibbard,
908 K., Olson, R., 2008. Global potential net primary production predicted from
909 vegetation class, precipitation, and temperature. Ecology 89, 2117-2126.
910 https://doi.org/10.1890/07-0850.1
911 Diéguez-Aranda, U., Rojo Alboreca, A., Castedo-Dorado, F., Álvarez González, J.G.,
912 Barrio-Anta, M., Crecente-Campo, F., González González, J.M., Pérez-Cruzado,
913 C., Rodríguez Soalleiro, R., López-Sánchez, C.A., Balboa-Murias, M.A., Gorgoso
914 Varela, J.J., Sánchez Rodríguez, F., 2009. Herramientas selvícolas para la gestión
915 forestal sostenible en Galicia. Consellería do Medio Rural, Xunta de Galicia,
916 Santiago de Compostela.

Fernandes, P., Loureiro, C., Botelho, H., Ferreira, A., Fernandes, M., 2002. Avaliaçao indirecta de carga de combustivel em Pinhal Bravo. Silva Lusit., 10, 73-90.

Fernandes, P.A.M., Loureiro, C., Botelho, H.S., 2004. Fire behaviour and severity in a maritime pine stand under differing fuel conditions. Ann. For. Sci., 61, 537–544. https://doi.org/10.1051/forest:2004048

Fernandes, P.M., Botelho, H.S., Rego, F.C., Loureiro, C., 2009. Empirical modelling of surface fire behaviour in maritime pine stands. Int. J. Wildland Fire 18, 698-710. https://doi.org/10.1071/WF08023

Fernandes, P.M., Rego, F.C., 1998. Equations for estimating fuel load in shrub communities dominated by *Chamaespartium tridentatum* and *Erica umbellata*, in: Viegas, D.X. (Ed.), Proceedings of the 3rd International Conference on Forest Fire Research and 14th Fire and Forest Meteorology Conference, Coimbra, pp. 16-20.

Fernandes, P.M., Rigolot, E., 2007. The fire ecology and management of maritime pine (*Pinus pinaster* Ait.). For. Ecol. Manage. 241, 1–13. https://doi.org/10.1016/j.foreco.2007.01.010

Fernández, C., Vega, J.A., Fonturbel, M.T., 2013. Shrub Resprouting Response after Fuel Reduction Treatments: Comparison of Prescribed Burning, Clearing and Mastication. J. Environ. Manage. 117, 235-241. https://doi.org/10.1016/j.jenvman.2013.01.004

Fernández-Alonso, J.M., Alberdi, I., Álvarez-González, J.G., Vega, J.A., Cañellas, I., Ruiz-González, A.D., 2013. Canopy fuel characteristics in relation to crown fire potential in pine stands: analysis, modelling and classification. Eur. J. For. Res. 132, 363–377. https://doi.org/10.1007/s10342-012-0680-z

941 Fonseca, T.F., Duarte, J.C., 2017. A silvicultural stand density model to control
942 understory in maritime pine stands. iForest 10, 829–836.
943 https://doi.org/10.3832/ifor2173-010
944 Friedman, J.H., 1991. Multivariate adaptive regression splines (with discussion). Ann.
945 Stat. 19, 1–141.
946 García Villabrille, J.D., 2015. Modelización del crecimiento y la producción de
947 plantaciones de *Eucalyptus globulus* Labill. en el noroeste de España. Ph.D.
948 Thesis. Universidad de Santiago de Compostela, Lugo.
949 Gaudio, N., Balandier, P., Marquier, A., 2008. Light-dependent development of two
950 competitive species (*Rubus idaeus*, *Cytisus scoparius*) colonizing gaps in temperate
951 forest. Ann. For. Sci. 65, 104. https://doi.org/10.1051/forest:2007076
952 Gómez-García, E., 2020. Estimating the changes in tree carbon stocks in Galician
953 forests (NW Spain) between 1972 and 2009. For. Ecol. Manage. 467, 118157.
954 https://doi.org/10.1016/j.foreco.2020.118157
955 Gómez-Vázquez, I., Crecente-Campo, F., Diéguez-Aranda, U., Castedo-Dorado, F.,
956 2013. Modelling canopy fuel variables in *Pinus pinaster* Ait. and *Pinus radiata* D.
957 Don stands in northwestern Spain. Ann. For. Sci. 70, 161-172.
958 https://doi.org/10.1007/s13595-012-0245-9
959 Gonzalez, M., Augusto, L., Gallet-Budynek, A., Xue, J., Yauschew-Raguenes, N.,
960 Guyon, D., Trichet, P., Delerue, F., Niollet, S., Andreasson, F., Achat, D.L.,
961 Bakker, M.R., 2013. Contribution of understory species to total ecosystem
962 aboveground and belowground biomass in temperate *Pinus pinaster* Ait. forests.
963 For. Ecol. Manage. 289, 38–47. https://doi.org/10.1016/j.foreco.2012.10.026
964 González-Hernández, M.P., Silva-Pando, F.J., Casal Jiménez, M., 1998. Production
965 patterns of understory layers in several Galician (NW Spain) woodlands.

966 Seasonality, net productivity and renewal rates. For. Ecol. Manage. 109, 251-259.
967 https://doi.org/10.1016/S0378-1127(98)00253-9
968 Graham, R.T., McCaffrey, S., Jain, T.B., 2004. Science basis for changing forest
969 structure to modify wildfire behavior and severity. USDA Forest Service Gen.
970 Tech. Rep. RMRS-GTR-120. Fort Collins, CO, USA. 43 p.
971 https://doi.org/10.2737/RMRS-GTR-120
972 Harmer, R., Kiewitt, A., Morgan, G., 2012. Can overstorey retention be used to control
973 bramble (*Rubus fruticosus* L. agg.) during regeneration of forests? Forestry 85,
974 135–144. https://doi.org/10.1093/forestry/cpr066
975 Heinrichs, S., Bernhardt-Roemermann, M., Schmidt, W., 2010. The estimation of
976 aboveground biomass and nutrient pools of understorey plants in closed Norway
977 spruce forests and on clearcuts. Eur. J. For. Res. 129, 613–624.
978 https://doi.org/10.1007/s10342-010-0362-7
979 Helms, J.A. 1998 The Dictionary of Forestry. Society of American Foresters, pp. 210.
980 Hosmer D.W., Lemeshow S., 2000. Applied Logistic Regression, 2nd ed., Wiley, New
981 York.
982 Hough, W.A., Albini, F.A., 1978. Predicting fire behavior in palmetto-gallberry fuel
983 complexes. Research Paper SE-RP-174. Asheville, NC: USDA-Forest Service,
984 Southeastern Forest Experiment Station. 48 p., 174, 1-48.
985 Huff, S., Ritchie, M., Temesgen, H., 2017. Allometric equations for estimating
986 aboveground biomass for common shrubs in northeastern California. For. Ecol.
987 Manage. 398, 48-63. https://doi.org/10.1016/j.foreco.2017.04.027
988 Johnson, K.D., Domke, G.M., Russell, M.B., Walters, B., Hom, J., Peduzzi, A.,
989 Birdsey, R., Dolan, K., Huang, W., 2017. Estimating aboveground live understory

vegetation carbon in the United States. Environ. Res. Lett. 12, 125010. https://doi.org/10.1088/1748-9326/aa8fdb

Keane, R.E., 2015. Wildland Fuel Fundamentals and Applications. Springer, Switzerland.

Keane, R.E., Reinhardt, E.D., Scott, J., Gray, K., Reardon, J., 2005. Estimating forest canopy bulk density using six indirect methods. Can. J. For. Res. 35, 724–739. https://doi.org/10.1139/x04-213

Keeley, J.E., Zedler, P.H., 1998. Evolution of life histories in *Pinus*, in: Richardson, D.M. (Ed.), Ecology and Biogeography of *Pinus*, Cambridge University Press, Cambridge, pp. 219– 250.

Kerns, B.K., Ohmann, J.L., 2004. Evaluation and prediction of shrub cover in coastal Oregon forests (USA). Ecol. Indic. 4, 83-98. https://doi.org/10.1016/j.ecolind.2003.12.002

Knowles, R.L., Horvath, G.C., Carter, M.A., Hawke, M.F., 1999. Developing a canopy closure model to predict overstorey/understorey relationships in *Pinus radiata* silvopastoral systems, in: Auclair, D., Dupraz, C. (Eds.), Agroforestry for Sustainable Land-Use Fundamental Research and Modelling with Emphasis on Temperate and Mediterranean Applications, Springer, pp. 109-119.

Landuyt, D., Maes, S.L., Depauw, L., Ampoorter, E., Blondeel, H., Perring, M.P., Brūmelis, G., Brunet, J., Decocq, G., Ouden, J., Härdtle, W., Hédl, R., Heinken, T., Heinrichs, S., Jaroszewicz, B., Kirby, K.J., Kopecký, M., Máliš, F., Wulf, M., Verheyen, K., 2019. Drivers of above-ground understorey biomass and nutrient stocks in temperate deciduous forests. J. Ecol. 108, 982-997. https://doi.org/10.1111/1365-2745.13318

1014 Légaré, S., Bergeron, Y., Leduc, A., Paré, D., 2001. Comparison of the understory
1015 vegetation in boreal forest types of southwest Quebec. Can. J. Bot., 79, 1019-
1016 1027. https://doi.org/10.1139/b01-076
1017 Levers, C., Verkerk, P.J., Müller, D., Verburg, P.H., Butsic, V., Leitão, P.J., Lindner,
1018 M., Kuemmerle, T., 2014. Drivers of forest harvesting intensity patterns in
1019 Europe. For. Ecol. Manage. 315, 160-172.
1020 http://dx.doi.org/10.1016/j.foreco.2013.12.030
1021 Lopes, D.M., Walford, N., Viana, H., Sette Jr., C.R., 2016. A proposed methodology for
1022 the correction of the leaf area index measured with a ceptometer for pinus and
1023 eucalyptus forests. Revista Árvore 40, 845-854. http://dx.doi.org/10.1590/0100-
1024 67622016000500008
1025 López-Senespleda, E., Calama, R., Ruiz-Peinado, R., 2021. Estimating forest floor
1026 carbon stocks in woodland formations in Spain. Sci. Tot. Environ. 788, 147734.
1027 https://doi.org/10.1016/j.scitotenv.2021.147734
1028 MAGRAMA, 2012a. Cuarto Inventario Forestal Nacional. Principado de Asturias.
1029 Dirección General de Desarrollo Rural y Política Forestal. Ministerio de
1030 Agricultura, Alimentación y Medio Ambiente.
1031 MAGRAMA, 2012b. Cuarto Inventario Forestal Nacional. Cantabria. Dirección
1032 General de Desarrollo Rural y Política Forestal. Ministerio de Agricultura,
1033 Alimentación y Medio Ambiente.
1034 MAGRAMA, 2013. Cuarto Inventario Forestal Nacional. Comunidad Autónoma del
1035 País Vasco / Euskadi. Dirección General de Desarrollo Rural y Política Forestal.
1036 Ministerio de Agricultura, Alimentación y Medio Ambiente

MAPA, 2019a. Anuario de estadística Forestal. Ministerio de Agricultura, Pesca y Alimentación. Gobierno de España. https://www.mapa.gob.es/es/desarrollo-rural/estadisticas/forestal_anuarios_todos.aspx (accessed 13 March 2023).

MAPA, 2019b. Los incendios forestales en España. Decenio 2006-2015. Ministerio de Agricultura, Pesca y Alimentación Secretaría General Técnica. 157 pp, Madrid.

MARM, 2011. Cuarto Inventario Forestal Nacional. Comunidad Autónoma de Galicia. Dirección General del Medio Natural y Política Forestal. Madrid.

McKenzie, D., Halpern, C.B., Nelson, C.R., 2000. Overstory influences on herb and shrub communities in mature forests of western Washington, U.S.A. Can. J. For. Res. 30, 1655-1666. https://doi.org/10.1139/x00-091

Messier, C., Parent, S., Bergeron, Y., 1998. Effects of overstory and understory vegetation on the understory light environment in mixed boreal forests. J. Veg. Sci. 9, 511–520. https://doi.org/10.2307/3237266

Milborrow, S., 2023. earth: Multivariate Adaptive Regression Splines. R package version 5.3.2. Derived from mda: mars by Hastie, T. and Tibshirani, R. Uses Alan Miller's Fortran utilities with Thomas Lumley's leaps wrapper. https://cran.r-project.org/package=earth (accessed 03 March 2023).

Mirra, I.M., Oliveira, T.M., Barros, A.M., Fernandes, P.M., 2017. Fuel dynamics following fire hazard reduction treatments in blue gum (*Eucalyptus globulus*) plantations in Portugal. For. Ecol. Manage. 398, 185-195. https://doi.org/10.1016/j.foreco.2017.05.016

Mitsopoulos, I., Xanthopoulos, G., 2016. Effect of stand, topographic, and climatic factors on the fuel complex characteristics of Aleppo (*Pinus halepensis* Mill.) and Calabrian (*Pinus brutia* Ten.) pine forests of Greece. For. Ecol. Manage. 360, 110-121. https://doi.org/10.1016/j.foreco.2015.10.027

1062 Mitsopoulos, I.D., Dimitrakopoulos, A.P., 2014. Estimation of canopy fuel
1063 characteristics of Aleppo pine (*Pinus halepensis* Mill.) forests in Greece based on
1064 common stand parameters. Eur. J. For. Res. 133, 73-79.
1065 https://doi.org/10.1007/s10342-013-0740-z
1066 Monserud R.A., 1976. Simulation of forest tree mortality. For. Sci. 22, 438–444.
1067 https://doi.org/10.1093/forestscience/22.4.438
1068 Montero, G., López-Leiva, C., Ruiz-Peinado, R., López-Senespleda, E., Onrubia, R.,
1069 Pasalodos, M., 2020. Producción de biomasa y fijación de carbono por los
1070 matorrales españoles y por el horizonte orgánico superficial de los suelos forestales.
1071 Ministerio de Agricultura, Pesca y Alimentación. Madrid.
1072 Montero, G., Ruiz-Peinado, R., Muñoz, M., 2005. Producción de biomasa y fijación de
1073 CO_2 por los bosques españoles. Monografía INIA: Serie Forestal 13. Instituto
1074 Nacional de Investigación y Tecnología Agraria y Alimentaria, Madrid.
1075 Moreno, J.M., Pineda, F.D., Rivas-Martínez, S., 1990. Climate and vegetation at the
1076 Eurosiberian-Mediterranean boundary in the Iberian Peninsula. J. Veg. Sci. 1, 233–
1077 244. https://doi.org/10.2307/3235660
1078 Nolan, R.H., Price, O.F., Samson, S.A., Jenkins, M.E., Rahmani, S., Boer, M.M., 2022.
1079 Framework for assessing live fine fuel loads and biomass consumption during fire.
1080 For. Ecol. Manage. 504, 119830. https://doi.org/10.1016/j.foreco.2021.119830
1081 Nunes, L., Álvarez-González, J.G., Alberdi, I., Silva, V., Rocha, M., Castro Rego, F.,
1082 2019. Analysis of the occurrence of wildfires in the Iberian Peninsula based on
1083 harmonised data from national forest inventories. Ann. For. Sci. 76, 27.
1084 https://doi.org/10.1007/s13595-019-0811-5
1085 Nunes, L., Moreno, M., Alberdi, I., Álvarez-González, J.G., Godinho-Ferreira, P.,
1086 Mazzoleni, S., Castro Rego, F., 2020. Harmonized classification of forest types in

1087 the Iberian Peninsula based on national forest inventories. Forests 11, 1170.
1088 https://doi.org/10.3390/f11111170
1089 Nunes, L., Pasalodos-Tato, M., Alberdi, I., Sequeira, A.C., Vega, J.A., Silva, V., Vieira,
1090 P., Castro Rego, F., 2022. Bulk density of shrub types and tree crowns to use with
1091 forest inventories in the Iberian Peninsula. Forests 13, 555.
1092 https://doi.org/10.3390/f13040555
1093 Oliveira, S., Oehler, F., San-Miguel-Ayanz, J., Camia, A., Pereira, J.M., 2012.
1094 Modeling spatial patterns of fire occurrence in Mediterranean Europe using
1095 Multiple Regression and Random Forest. For. Ecol. Manage. 275, 117-129.
1096 http://dx.doi.org/10.1016/j.foreco.2012.03.003
1097 Olson, C.M., Martin, R.E., 1981. Estimating biomass of shrubs and forbs in central
1098 Washington Douglas-fir stands. Res. Note PNW-RN-380. Portland, OR: USDA
1099 Forest Service, Pacific Northwest Forest and Range Experiment Station.
1100 Onaindia, M., Ametzaga-Arregi, I., San Sebastián, M., Mitxelena, A., Rodríguez-
1101 Loinaz, G., Peña, L., Alday, J.G., 2013. Can understorey native woodland plant
1102 species regenerate under exotic pine plantations using natural succession? For.
1103 Ecol. Manage. 308, 136-144. https://doi.org/10.1016/j.foreco.2013.07.046
1104 Parresol, B.R., Blake, J.I., Thompson, A.J., 2012. Effects of overstory composition and
1105 prescribed fire on fuel loading across a heterogeneous managed landscape in the
1106 southeastern USA. For. Ecol. Manage. 273, 29–42.
1107 https://doi.org/10.1016/j.foreco.2011.08.003
1108 Pasalodos-Tato, M.; Ruiz-Peinado, R., del Río, M., Montero, G., 2015. Shrub biomass
1109 accumulation and growth rate models to quantify carbon stocks and fluxes for the
1110 Mediterranean region. Eur. J. For. Res. 134, 537–553.
1111 https://doi.org/10.1007/s10342-015-0870-6

1112 Pausas, J.G., Paula, S., 2012. Fuel shapes the fire–climate relationship: evidence from
1113 Mediterranean ecosystems. Glob. Ecol. Biogeogr. 21, 1074-1082.
1114 https://doi.org/10.1111/j.1466-8238.2012.00769.x
1115 Pearce, H.G., Anderson, W.R., Fogarty, L.G., Todoroki, C.L., Anderson, S.A.J., 2010.
1116 Linear mixed-effects models for estimating biomass and fuel loads in shrublands.
1117 Can. J. For. Res. 40, 2015–2026. https://doi.org/10.1139/X10-139
1118 Piqué, M., González-Olabarria, J.R., Busquets, E., 2022. Dynamic evaluation of early
1119 silvicultural treatments for wildfire prevention. Forests 13, 858.
1120 https://doi.org/10.3390/f13060858
1121 Porté, A.J., Samalens, J-C., Dulhoste, R., Teissier Du Cros, R., Bosc, A., Meredieu, C.,
1122 2009. Using cover measurements to estimate aboveground understorey biomass in
1123 Maritime pine stands. Ann. For. Sci. 66, 307.
1124 https://doi.org/10.1051/forest/2009005
1125 Pyne, S.J., Andrews, P.L., Laven, R.D., 1996. Introduction to wildland fire. 2nd edition.
1126 John Wiley & Sons, New York.
1127 R Core Team, 2022. R: A language and environment for statistical computing; R
1128 Foundation for Statistical Computing, Vienna, Austria. https://www.R-project.org/
1129 (accessed 03 March 2023).
1130 Rego, F.C., Morgan, P., Fernandes, P., Hoffman, C., 2021. Fuel and fire behavior
1131 description, in Fire Science, from Chemistry to Landscape Management. Springer
1132 Cham. https://doi.org/10.1007/978-3-030-69815-7
1133 Richards, F.J., 1959. A flexible growth function for empirical use. J. Exp. Bot. 10, 290–
1134 300. https://doi.org/10.1093/jxb/10.2.290
1135 Rodríguez Soalleiro, R.J., Madrigal, A., 2008. Selvicultura de *Pinus pinaster* Ait. subsp.
1136 atlantica H. de Vill., in: Serrada, R., Montero, G., Reque, J.A. (Eds.), Compendio

de selvicultura aplicada en España. Instituto Nacional de Investigación y Tecnología Agraria y Alimentaria. Madrid, pp. 367-398.

Rothermel, R.C., 1972. A Mathematical Model for Predicting Fire Spread in Widland Fuels, Res. Pap. INT-115. Ogden, UT.40 p.

Ruiz, F., López, G.A., Toval, G., Alejano, R., 2008. Selvicultura de *Eucalyptus globulus* Labill., in: Serrada, R., Montero, G., Reque, J.A. (Eds.), Compendio de selvicultura aplicada en España. Instituto Nacional de Investigación y Tecnología Agraria y Alimentaria. Madrid, pp. 117-154.

Ruiz-González, A.D., Castedo-Dorado, F., Vega, J.A., Jiménez, E., Fernández-Alonso, J. M., Álvarez-González, J.G., 2015. Modelling canopy fuel dynamics of maritime pine stands in north-west Spain. Int. J. Wildland Fire, 24, 92-102. https://doi.org/10.1071/WF14020

Ruiz-Peinado, Moreno, G., Juarez, E., Montero, G., Roig, S., 2015. The contribution of two common shrub species to aboveground and belowground carbon stock in Iberian dehesas. J. Arid. Environ. 91, 22-30. https://doi.org/10.1016/j.jaridenv.2012.11.002

Russell, M.B., D'Amato, A.W., Schulz, B.K., Woodall, C.W., Domke, G.M., Bradford, J.B., 2014. Quantifying understorey vegetation in the US Lake States: a proposed framework to inform regional forest carbon stocks. Forestry 87, 629-638. https://doi.org/10.1093/forestry/cpu023

Sánchez-Pinillos, M., De Cáceres, M., Casals, P., Alvarez, A., Beltrán, M., Pausas, J.G., Vayreda, J., Coll, L., 2021. Spatial and temporal variations of overstory and understorey fuels in Mediterranean landscapes. For. Ecol. Manage. 490, 119094. https://doi.org/10.1016/j.foreco.2021.119094

1161 Sands, P.J., Landsberg, J.J. 2002. Parameterisation of 3-PG for plantation grown
1162 *Eucalyptus globulus*. For. Ecol. Manage. 163, 273-292.
1163 San-Miguel-Ayanz, J., Durrant, T., Boca, R., Libertà, G., Branco, A., de Rigo, D.,
1164 Ferrari, D., Maianti, P., Artés, T., Costa, H., Lana, F., Löffler, P., Nuijten, D.,
1165 Ahlgren, A.C., Leray, T., 2018. Forest Fires in Europe, Middle East and North
1166 Africa 2017. EUR 29318 EN, Publications Office of the European Union,
1167 Luxembourg
1168 SAS Institute Inc. 2004. SAS/ETS© 9.1 User's Guide. Cary, NC: SAS Institute Inc.
1169 Scott, J.H., Reinhardt, E.D., 2001. Assessing crown fire potential by linking models of
1170 surface and crown fire behavior. Res. Pap. RMRS-RP-29. USDA Forest Service,
1171 Rocky Mountain Research Station, 59 p.
1172 Scott, J.H., Thompson, M.P., Calkin, D.E., 2013. A wildfire risk assessment framework
1173 for land and resource management. USDA Forest Service Gen. Tech. Rep. RMRS-
1174 GTR-315, 83 p. https://doi.org/10.2737/rmrs-gtr-315
1175 Serrada, R., Aroca, M.J., Roig, S., Bravo Fernández, A., Gómez, V., 2011. Impactos,
1176 vulnerabilidad y adaptación al cambio climático en el sector forestal. Notas sobre
1177 gestión adaptativa de las masas forestales ante el cambio climático. Ministerio de
1178 Medio Ambiente y Medio Rural y Marino, Secretaría General Técnica, Centro de
1179 Publicaciones, Madrid.
1180 Silva-Pando, F.J., Rozados Lorenzo, M.J., González Hernández, M.P., 2002. Grasslands
1181 and scrublands in the northwest of the Iberian Peninsula: Silvopastoral systems and
1182 nature conservation, in: Redecker, B., Härdtle, W., Finck, P., Riecken, U.,
1183 Schröder, E. (Eds.), Pasture Landscapes and Nature Conservation. Springer, Berlin.

1184 Suchar, V.A., Crookston, N.L., 2010. Understory cover and biomass indices predictions
1185 for forest ecosystems of the Northwestern United States. Ecol. Indic. 10, 602-609.
1186 https://doi.org/10.1016/j.ecolind.2009.10.004
1187 Tang, S., Li, Y., Wang, Y., 2001. Simultaneous equations, error-in-variable models, and
1188 model integration in systems ecology. Ecol. Model. 142, 285–294.
1189 https://doi.org/10.1016/S0304-3800(01)00326-X
1190 Tang, S., Zhang, H., Xu, H., 2000. Study on establish and estimate method of
1191 compatible biomass model. Sci. Silv. Sin. 36(Suppl.1):19 –27 (in Chinese with
1192 English abstract).
1193 Thompson, M.P., Haas, J.R., Gilbertson-Day, J.W., Scott, J.H., Langowski, P., Bowne,
1194 E., Calkin, D.E., 2015. Development and application of a geospatial wildfire
1195 exposure and risk calculation tool. Environ. Model. Softw., 63, 61–72.
1196 https://doi.org/10.1016/j.envsoft.2014.09.018
1197 Tomé, J., Tomé, M., Barreiro, S., Paulo, J.A., (2006). Age-independent difference
1198 equations for modeling tree and stand growth. Can. J. For. Res. 36, 1621–1630.
1199 https://doi.org/10.1139/x06-065
1200 Tomé, M., Almeida, M.H., Barreiro, S., Branco, M.R., Deus, E., Pinto, G., Silva, J.S.,
1201 Soares, P., Rodríguez-Soalleiro, R., 2021. Opportunities and challenges of
1202 Eucalyptus plantations in Europe: the Iberian Peninsula experience. Eur. J. For.
1203 Res. 140, 489-510. https://doi.org/10.1007/s10342-021-01358-z
1204 Uresk, D.W., Severson, K.E., 1989. Understory-overstory relationships in ponderosa
1205 pine forests, Black Hills, South Dakota. J. Range Manage. 42, 203–208.
1206 Valbuena-Carabaña, M., López de Heredia, U., Fuentes-Utrilla, P., González-Donce, I.,
1207 Gil, L. 2010. Historical and recent changes in the Spanish forests: A socio-

economic process. Rev. Palaeobot. Palynol. 162, 492-506. https://doi.org/10.1016/j.revpalbo.2009.11.003

Valladares, F., Laanisto, L., Niinemets, Ü, Zavala, M.A., 2016. Shedding light on shade: ecological perspectives of understorey plant life. Plant Ecol. Divers. 9, 237-251. https://doi.org/10.1080/17550874.2016.1210262

Van Wagner, C.E., 1977. Conditions for the start and spread of crown fire. Can. J. For. Res. 7, 23-34.

Vega, J.A., 2001. Efectos del fuego prescrito sobre el suelo en pinares de *Pinus pinaster* Ait. de Galicia. Ph.D. Thesis. Universidad Politécnica de Madrid, Madrid.

Vega, J.A., Arellano-Pérez, S., Álvarez-González, J.G., Fernández, C., Jiménez, E., Cuiñas, P., Fernández-Alonso, J.M., Vega-Nieva, D.J., Castedo-Dorado, F., Alonso-Rego, C., Fontúrbel, T., Ruiz-González, A.D., 2022a. Modelling fuel loads of understorey vegetation and forest floor components in pine stands in NW Spain. For. Ecosyst. 9, 100074. https://doi.org/10.1016/j.fecs.2022.100074

Vega, J.A., Arellano-Pérez, S., Álvarez-González, J.G., Fernández, C., Jiménez, E., Fernández-Alonso, J.M., Vega-Nieva, D.J., Briones-Herrera, C., Alonso-Rego, C., Fontúrbel, T., Ruiz-González, A.D., 2022b. Modelling aboveground biomass and fuel load components at stand level in shrub communities in NW Spain. For. Ecol. Manage. 505, 119926. https://doi.org/10.1016/j.foreco.2021.119926

Vega, J.A., Fontúrbel, T., Merino, A., Fernández, C., Ferreiro, A., Jiménez, E., 2013. Testing the ability of visual indicators of soil burn severity to reflect changes in soil chemical and microbial properties in pine forests and shrubland. Plant Soil 369, 73–91. https://doi.org/10.1007/s11104-012-1532-9

1231 Verkerk, P.J., Levers, C., Kuemmerle, T., Lindner, M., Valbuena, R., Verburg, P.H.,
1232 Zudin, S., 2015. Mapping wood production in European forests. Forest Ecol.
1233 Manage. 357, 228–238. https://doi.org/10.1016/j.foreco.2015.08.007
1234 Wagner, S., Fischer, H., Huth, F., 2011. Canopy effects on vegetation caused by
1235 harvesting and regeneration treatments. Eur. J. For. Res. 130, 17-40.
1236 https://doi.org/10.1007/s10342-010-0378-z
1237 White, A.S., Cook, J.E., Vose, J.M., 1991. Effects of fire and stand structure on grass
1238 phenology in a ponderosa pine forest. Am. Midl. Naturalist 126, 269–278.
1239 https://doi.org/10.2307/2426102
1240 Xanthopoulos, G., Manasi, M.A., 2002. Practical Methodology for the Development of
1241 Shrub Fuel Models for Fire Behavior Prediction, in: Viegas, D.X. (Ed.),
1242 Proceedings of the IV International Conference on Forest Fire Research 2002,
1243 Wildland Fire Safety Summit, Millpress, Rotterdam, pp. 1-12.

Supplementary material

Models for estimating understorey fuel loads from understorey metrics

The database comprised 177 destructive understorey sampling plots established in pure and even-aged stands of the three pine species (112 of *P. pinaster*, 32 of *P. radiata* and 33 of *P. sylvestris*) covering a relatively wide range of the main attributes of these type of forests in Galicia. A complete description of the database used and the measurements made can be found in Vega et al. (2022a). The mean value and standard deviation of the main overstorey and understorey variables of the 177 sample plots used to fit the systems of equations for estimating understorey shrub fuel loads are shown in Table S1.

Table S1. Mean values and standard deviations (in brackets) of the main overstorey and understorey variables of the 177 sample plots used to fit the systems of equations for estimating understorey shrub fuel loads distinguished by pine species.

Variable	*Pinus pinaster* n = 112	*Pinus radiata* n = 32	*Pinus sylvestris* n = 33
$\bar{d}$ (cm)	18.44 (4.69)	20.34 (8.35)	18.70 (5.00)
$\bar{h}$ (m)	12.25 (3.43)	14.14 (5.78)	12.28 (2.71)
N (stems/ha)	1455.00 (1071.07)	849.04 (420.15)	998.70 (352.27)
G (m^2/ha)	36.55 (10.67)	37.47 (18.22)	38.91 (15.55)
CC (%)	63.92 (11.03)	49.39 (17.08)	58.95 (11.18)
Cov_{shr} (%)	61.75 (28.79)	82.84 (21.32)	75.59 (19.54)
$\overline{h_{shr}}$ (cm)	77.47 (38.44)	75.62 (39.77)	65.10 (20.74)
W_{shr}(kg/m^2)	0.9042 (0.6079)	1.6486 (1.0136)	1.4255 (0.8633)
W_{shr_G23} (kg/m^2)	0.2954 (0.3103)	0.4915 (0.3561)	0.5108 (0.3292)
W_{shr_G1} (kg/m^2)	0.6089 (0.4080)	1.1571 (0.7496)	0.9148 (0.6094)
$W_{shr\_G1\_dead}$ (kg/m^2)	0.3794 (0.2681)	0.7240 (0.5101)	0.5466 (0.3628)
$W_{shr\_G1\_live}$ (kg/m^2)	0.2295 (0.1801)	0.4331 (0.2695)	0.3682 (0.2595)

The system used to estimate the total shrub load (W_{shr}) is composed of five compatible equations for the following: the coarse shrub fuel load (W_{shr_G23}; 0.6 cm ≤ diameter < 7.5 cm); the fine shrub fuel load (W_{shr_G1}, diameter < 0.6 cm); and the dead fine and live fine shrub loads ($W_{shr\_G1\_dead}$ and $W_{shr\_G1\_live}$, respectively). The equations must satisfy the additivity property, i.e. the sum of the fuel loads estimated for each fraction separately must equal the biomass estimated by the total fuel load equation; the same is true for the fine load fractions relative to the total fine load. To ensure additivity, the system was fitted simultaneously and consists of the following equations (Tang et al., 2000, 2001):

$$\widehat{W_{shr}} = a_0 \overline{h_{shr}}^{a_1} Cov_{shr\_bliss}^{a_2} \tag{S1}$$

$$\widehat{W_{shr\_G23}} = \frac{\widehat{W_{shr}}}{1 + \exp\left[b_0 + b_1 \ln\left(\overline{h_{shr}}\right) + b_2 \ln\left(Cov_{shr\_Bliss}\right)\right]} \tag{S2}$$

$$\widehat{W_{shr\_G1}} = \frac{\widehat{W_{shr}} \cdot \exp\left[b_0 + b_1 \ln\left(\overline{h_{shr}}\right) + b_2 \ln\left(Cov_{shr\_Bliss}\right)\right]}{1 + \exp\left[b_0 + b_1 \ln\left(\overline{h_{shr}}\right) + b_2 \ln\left(Cov_{shr\_Bliss}\right)\right]} \tag{S3}$$

$$\widehat{W_{shr\_G1\_dead}} = \frac{\widehat{W_{shr\_G1}}}{1 + \exp\left[c_0 + c_i \ln\left(Cov_{shr\_Bliss}\right)\right]} \tag{S4}$$

$$\widehat{W_{shr\_G1\_live}} = \frac{\widehat{W_{shr\_G1}} \exp\left[c_0 + c_i \ln\left(Cov_{shr\_Bliss}\right)\right]}{1 + \exp\left[c_0 + c_i \ln\left(Cov_{shr\_Bliss}\right)\right]} \tag{S5}$$

where W_{shr} and W_{shr_Gi} are the total and component shrub fuel loads (kg/m^2), respectively, $\overline{h_{shr}}$ is the mean shrub height (cm), "ln" is the natural logarithm; Cov_{shr_Bliss} is an arcsine-square root transformation of the shrub cover (Cov_{shr}, %) to stabilize the variance and improve normality (Bliss, 1938) and a_i, b_i and c_i are parameters to be estimated.

The systems of equations (S1 to S5) were fitted simultaneously by nonlinear seemingly unrelated regression (NLSUR), which considers the cross-equation correlations. Model fitting was carried out using the MODEL procedure of SAS/ETS® (SAS Institute Inc., 2004). Two goodness-of fit statistics were used to check the accuracy of estimates: model efficiency (ME) and root mean square error (RMSE).

$$\mathrm{ME} = 1 - \frac{\sum_{i=1}^{n}\left(Y_i - \widehat{Y}_i\right)^2}{\sum_{i=1}^{n}(Y_i - \bar{Y})^2} \tag{S6}$$

$$\mathrm{RMSE} = \sqrt{\frac{\sum_{i=1}^{n}\left(Y_i - \widehat{Y}_i\right)^2}{n-1}} \tag{S7}$$

where Y_i, $\widehat{Y}_i$ and $\bar{Y}$ are the observed, predicted and mean values of the dependent variable and n is the number of observations used to fit the equation.

The mathematical expressions of the compatible equations fitted for the understorey fuel loads as well as with the values of the goodness-of-fit statistics are shown in Table S2. All parameters were significant (α = 0.05), and no multicollinearity problems were observed. The values and signs of all the parameters were biologically consistent, and graphical inspection of the studentized residuals showed random patterns of residuals around zero with homogeneous variance and no discernible trends.

Table S2. Mathematical expressions of the compatible equations fitted to estimate understorey fuel loads by fuel fractions based on understorey metrics. W_{shr} = total shrub fuel load, W_{shr_G23} = coarse shrub fuel load, W_{shr_G1} = fine shrub fuel load, $W_{shr\_G1\_dead}$ = dead fine shrub fuel load and $W_{shr\_G1\_live}$ = live fine shrub fuel load.

Equation system for estimating understorey fuel loads based on understorey metrics
$\widehat{W_{shr}} = 0.0734 \cdot \overline{h_{shr}}^{0.6268} \cdot Cov_{shr\_Bliss}^{1.4818}$
ME = 0.5676 RMSE = 0.5290 kg/m^2
$\widehat{W_{shr\_G23}} = \frac{\widehat{W_{shr}}}{1 + \exp\left[1.9440 - 0.3027\ln\left(\overline{h_{shr}}\right) + 0.6449\ln\left(Cov_{shr\_Bliss}\right)\right]}$
ME = 0.3848 RMSE = 0.2633 kg/m^2
$\widehat{W_{shr\_G1}} = \frac{\widehat{W_{shr}}\exp\left[1.9440 - 0.3027\ln\left(\overline{h_{shr}}\right) + 0.6449\ln\left(Cov_{shr\_Bliss}\right)\right]}{1 + \exp\left[1.9440 - 0.3027\ln\left(\overline{h_{shr}}\right) + 0.6449\ln\left(Cov_{shr\_Bliss}\right)\right]}$
ME = 0.5175 RMSE = 0.3924 kg/m^2
$\widehat{W_{shr\_G1\_dead}} = \frac{\widehat{W_{shr\_G1}}}{1 + \exp\left[1.5582\ln\left(Cov_{Shr\_Bliss}\right)\right]}$
ME = 0.3798 RMSE = 0.1808 kg/m^2
$\widehat{W_{shr\_G1\_live}} = \frac{\widehat{W_{shr\_G1}}\exp\left[1.5582\ln\left(Cov_{shr\_Bliss}\right)\right]}{1 + \exp\left[1.5582\ln\left(Cov_{shr\_Bliss}\right)\right]}$
ME = 0.4219 RMSE = 0.2774 kg/m^2

The fitted equations explained between 38% and 57% of the observed variability in $W_{shr\_G1\_dead}$ and W_{shr}, respectively. The equation used to estimate W_{shr_G1} explained 52% of the observed variability. These values are within the ranges found in other studies of understorey fuel load quantification at stand level (e.g. Hough and Albini, 1978; Fernandes and Rego, 1998; Porte et al., 2009; Russell et al., 2014; Pasalodos-Tato et al., 2015; Nolan et al., 2022). The results are somewhat less accurate than those reported by Vega et al. (2022a) for the same database and using both understorey and overstorey variables as regressors. The poorer results obtained in the present study were, to a certain extent, predictable, since the overstorey variables are known to explain a large part of the observed variability in the understorey fuels (e.g., Kerns and Ohmann, 2004; Mitsopoulos and Xanthopoulos, 2016).

The system of shrub fuel load equations depends only on one or two regressors characterizing the understorey layer ($\overline{h_{shr}}$ and Cov_{shr_Bliss}). These two variables were the only ones available regarding the shrub species in the SNFI database and have been widely used in models for understorey load estimation as individual variables or as phytovolume (defined as the combined understory cover times height; e.g., Olson and Martin, 1981; Fernandes et al., 2002; Xanthopoluos and Manasi, 2002; Heinrichs et al., 2010; Pearce et al., 2010; Gonzalez et al., 2013; Ruiz-Peinado et al., 2015). Moreover, the use of individual plant variables such as crown area (Huff et al., 2017; De Cáceres et al., 2019) and shrub stem diameter (Nolan et al., 2022) would not be feasible for shrubland formations in the study area, because the understorey is frequently composed of multi-stemmed plants with intermingled crowns, so that measurement of individual plant variables would be unfeasible or very costly.

References cited in Supplementary material:

Bliss, C., 1938. The transformation of percentages for use in the analysis of variance. Ohio J. Sci. 38, 9–12.

De Cáceres, M., Casals, P., Gabriel, E., Castro, X., 2019. Scaling-up individual-level allometric equations to predict stand-level fuel loading in Mediterranean shrublands. Ann. For. Sci. 76, 87. https://doi.org/10.1007/s13595-019-0873-4

Fernandes, P., Loureiro, C., Botelho, H., Ferreira, A., Fernandes, M., 2002. Avaliaçao indirecta de carga de combustivel em Pinhal Bravo. Silva Lusit., 10, 73-90.

Fernandes, P.M., Rego, F.C., 1998. Equations for estimating fuel load in shrub communities dominated by *Chamaespartium tridentatum* and *Erica umbellata*, in: Viegas, D.X. (Ed.), Proceedings of the 3rd International Conference on Forest Fire Research and 14th Fire and Forest Meteorology Conference, Coimbra, pp. 16-20.

Gonzalez, M., Augusto, L., Gallet-Budynek, A., Xue, J., Yauschew-Raguenes, N., Guyon, D., Trichet, P., Delerue, F., Niollet, S., Andreasson, F., Achat, D.L., Bakker, M.R., 2013. Contribution of understory species to total ecosystem aboveground and belowground biomass in temperate *Pinus pinaster* Ait. forests. For. Ecol. Manage. 289, 38–47. https://doi.org/10.1016/j.foreco.2012.10.026

Heinrichs, S., Bernhardt-Roemermann, M., Schmidt, W., 2010. The estimation of aboveground biomass and nutrient pools of understorey plants in closed Norway spruce forests and on clearcuts. Eur. J. For. Res. 129, 613–624. https://doi.org/10.1007/s10342-010-0362-7

Hough, W.A., Albini, F.A., 1978. Predicting fire behavior in palmetto-gallberry fuel complexes. Research Paper SE-RP-174. Asheville, NC: USDA-Forest Service, Southeastern Forest Experiment Station. 48 p., 174, 1-48.

Huff, S., Ritchie, M., Temesgen, H., 2017. Allometric equations for estimating aboveground biomass for common shrubs in northeastern California. For. Ecol. Manage. 398, 48-63. https://doi.org/10.1016/j.foreco.2017.04.027

Kerns, B.K., Ohmann, J.L., 2004. Evaluation and prediction of shrub cover in coastal Oregon forests (USA). Ecol. Indic. 4, 83-98. https://doi.org/10.1016/j.ecolind.2003.12.002

Mitsopoulos, I., Xanthopoulos, G., 2016. Effect of stand, topographic, and climatic factors on the fuel complex characteristics of Aleppo (*Pinus halepensis* Mill.) and Calabrian (*Pinus brutia* Ten.) pine forests of Greece. For. Ecol. Manage. 360, 110-121. https://doi.org/10.1016/j.foreco.2015.10.027

Nolan, R.H., Price, O.F., Samson, S.A., Jenkins, M.E., Rahmani, S., Boer, M.M., 2022. Framework for assessing live fine fuel loads and biomass consumption during fire. For. Ecol. Manage. 504, 119830. https://doi.org/10.1016/j.foreco.2021.119830

Nolan, R.H., Price, O.F., Samson, S.A., Jenkins, M.E., Rahmani, S., Boer, M.M., 2022. Framework for assessing live fine fuel loads and biomass consumption during fire. For. Ecol. Manage. 504, 119830. https://doi.org/10.1016/j.foreco.2021.119830

Olson, C.M., Martin, R.E., 1981. Estimating biomass of shrubs and forbs in central Washington Douglas-fir stands. Res. Note PNW-RN-380. Portland, OR: USDA Forest Service, Pacific Northwest Forest and Range Experiment Station.

Pasalodos-Tato, M.; Ruiz-Peinado, R., del Río, M., Montero, G., 2015. Shrub biomass accumulation and growth rate models to quantify carbon stocks and fluxes for the Mediterranean region. Eur. J. For. Res. 134, 537–553. https://doi.org/10.1007/s10342-015-0870-6

Pearce, H.G., Anderson, W.R., Fogarty, L.G., Todoroki, C.L., Anderson, S.A.J., 2010. Linear mixed-effects models for estimating biomass and fuel loads in shrublands. Can. J. For. Res. 40, 2015–2026. https://doi.org/10.1139/X10-139

Porté, A.J., Samalens, J-C., Dulhoste, R., Teissier Du Cros, R., Bosc, A., Meredieu, C., 2009. Using cover measurements to estimate aboveground understorey biomass in Maritime pine stands. Ann. For. Sci. 66, 307. https://doi.org/10.1051/forest/2009005

Ruiz-Peinado, Moreno, G., Juarez, E., Montero, G., Roig, S., 2015. The contribution of two common shrub species to aboveground and belowground carbon stock in Iberian dehesas. J. Arid. Environ. 91, 22-30. https://doi.org/10.1016/j.jaridenv.2012.11.002

Russell, M.B., D'Amato, A.W., Schulz, B.K., Woodall, C.W., Domke, G.M., Bradford, J.B., 2014. Quantifying understorey vegetation in the US Lake States: a proposed framework to inform regional forest carbon stocks. Forestry 87, 629-638. https://doi.org/10.1093/forestry/cpu023

SAS Institute Inc. 2004. SAS/ETS© 9.1 User's Guide. Cary, NC: SAS Institute Inc.

Tang, S., Li, Y., Wang, Y., 2001. Simultaneous equations, error-in-variable models, and model integration in systems ecology. Ecol. Model. 142, 285–294. https://doi.org/10.1016/S0304-3800(01)00326-X

Tang, S., Zhang, H., Xu, H., 2000. Study on establish and estimate method of compatible biomass model. Sci. Silv. Sin. 36(Suppl.1):19 –27 (in Chinese with English abstract).

Vega, J.A., Arellano-Pérez, S., Álvarez-González, J.G., Fernández, C., Jiménez, E., Cuiñas, P., Fernández-Alonso, J.M., Vega-Nieva, D.J., Castedo-Dorado, F., Alonso-Rego, C., Fontúrbel, T., Ruiz-González, A.D., 2022a. Modelling fuel loads of understorey vegetation and forest floor components in pine stands in NW Spain. For. Ecosyst. 9, 100074. https://doi.org/10.1016/j.fecs.2022.100074

Xanthopoulos, G., Manasi, M.A., 2002. Practical Methodology for the Development of Shrub Fuel Models for Fire Behavior Prediction, in: Viegas, D.X. (Ed.), Proceedings of the IV International Conference on Forest Fire Research 2002, Wildland Fire Safety Summit, Millpress, Rotterdam, pp. 1-12.